Int. J. Heat Mass Transfer. Vol. 7, pp. 1151–1174. Pergamon Press 1964. Printed in Great Britain

HIGHLY NONEQUILIBRIUM BOUNDARY-LAYER FLOWS OF A MULTICOMPONENT DISSOCIATED GAS MIXTURE†

G. R. INGER‡
Aerospace Corporation, El Segundo, California

(*Received* 23 *January* 1964 *and in revised form* 15 *April* 1964)

Abstract—Analytical solutions are presented for a family of highly nonequilibrium (nearly frozen) boundary-layer flows of a four-component dissociated gas mixture around non-ablating bodies with either a completely catalytic or perfectly non-catalytic surface. Both self-similar and locally non-similar flows are studied for either recombination rate controlled or dissociation rate controlled situations. The nonequilibrium boundary-layer behavior, including the sensitivity to the various chemical kinetic data and transport property parameters, is considered in detail for highly cooled stagnation point flows on blunt bodies and hypersonic flows over sharp flat plates and slender cones. The accuracy of the local similarity approximation and use of nonequilibrium binary scaling laws are also examined for the plate and cone flows.

NOMENCLATURE

A_i, dissociation rate parameter, see equation (7);
C, Chapman–Rubesin parameter $(\rho\mu/\rho_e\mu_e)$;
$\overline{c_P}$, specific heat of mixture;
$f(\eta)$, boundary-layer stream function;
G_i, reaction rate function, equations (9) and (10);
$\bar{H}_D$, averaged heat of formation for atoms, equation (15);
H_{D_i}, $h^0_{f_i}/\overline{c_P}\,T_e$;
$h^0_{f_i}$, heat of formation of i-th chemical specie;
I_s, integral function defined by equation (29);
$\mathscr{I}_i, \bar{\mathscr{I}}_i$, reaction rate integrals; equations (30a) and (35b), respectively;
$I(\eta, Sc)$, $\int_0^\eta \exp\left(-Sc\int_0^\eta f\,\mathrm{d}\eta\right)\mathrm{d}\eta$;
J, switching symbol, see equation (26);
k_{D_i}, dissociation rate;
k_{R_i}, recombination rate;
k'_{R_i}, recombination rate constant $(k_{R_i} = k'_{R_i}\,T^{\omega})$;
Le, Lewis number (Pr/Sc);
M, exponent in the relation $u_e \sim x^M$ for incompressible wedge flows;
M_∞, free stream Mach number;
m_i, molecular weight of i-th chemical specie;
m_m, molecular weight of undissociated gas mixture;
N, $\sum N_i$;
N_i, mole fraction of i-th chemical specie;
Pr, Prandtl number;
p, static pressure;
p_0, atmospheric pressure;
p_{D_i}, characteristic dissociation pressure, see equation (7);
Q, $(\xi/\Gamma)\,(\mathrm{d}\Gamma/\mathrm{d}\xi)$;
Q_w, Heat-transfer rate function;
q_w, heat-transfer rate;
$\mathscr{R}_u$, universal gas constant;
r_B, local body radius in transverse plane;
Sc, Schmidt number;
s_i, dissociation rate parameter; equation (7);
$\mathbf{s}(\eta)$, function defined by equation (27);
T, absolute temperature;
T_{D_i}, characteristic dissociation temperature for i-th atom;
T_{R_1}, T_{R_2}, reference temperatures in reaction rate equations;

† This paper was prepared under U.S. Air Force Contract No. AF 04(695)-269.
‡ Member, Technical Staff, Aerodynamics and Propulsion Research Laboratories.

U, $u_e^2/2\,\overline{c_P}\,T_e$;
u, local velocity component parallel to body;
$\dot{w}_i$, net rate of i-th specie mass destruction due to chemical reaction;
$\dot{w}_Z$, total reaction source term for atoms ($=\sum_{\text{atoms}} \dot{w}_i$), equation (13);
x, y, co-ordinates parallel and normal to body, respectively;
Z, a/a_e;
z_i, a_i/a_{ie};
a, total atom mass fraction ($=\sum_{\text{atoms}} a_i$);
a_i, mass fraction of i-th chemical specie;
β_i^*, parameter defined in equation (33);
Γ, characteristic (flow-time/recombination-time) ratio, equation (12);
Γ_D, characteristic (flow-time/dissociation-time) ratio, equation (39);
δ, wedge or cone half-angle;
ϵ, body shape factor ($=0$, two-dimensional, $=1$, axisymmetric);
η, boundary-layer similarity co-ordinate, equation (1);
η^*, location of maximum temperature;
θ, T/T_e;
θ_{D_i}, T_{D_i}/T_e;
$\theta_P(\eta, Pr)$, $2\,Pr\int_0^\eta (f'')^{Pr}\left[\int_0^\eta (f'')^{2-Pr}\,d\eta\right]d\eta$;
κ, body-shape inviscid-flow factor $[(x/\xi)\,d\xi/dx]$;
λ_i, $\overline{\lambda_i}$, recombination rate parameters, equations (9) and (10);
μ, coefficient of viscosity;
ξ, boundary-layer similarity co-ordinate, equation (1);
ρ, density of mixture;
ψ, boundary-layer stream function;
ω_i, ω, recombination rate temperature-dependence exponent.

Subscripts

a, denotes atom;
B, denotes quantity based on Blasius velocity distribution;
e, local inviscid flow conditions at edge of boundary layer;
F, chemically frozen boundary-layer solution;
I, denotes first-order nonequilibrium reaction effect (nearly frozen flow);
i, i-th chemical specie ($i = 1, 2, 3, 4$ herein);
m, denotes molecule;
w, conditions at body surface;
∞, free stream conditions.

INTRODUCTION

IT IS WELL established that appreciable departures from chemical equilibrium will occur in the dissociated gas flow around blunt-nosed or slender, sharp-nosed reentry bodies at hypersonic flight speeds and high altitudes [1–7]. Consequently, there is considerable interest in the theory of nonequilibrium-dissociated laminar boundary-layer flows in connection with reentry technology studies. A detailed theoretical knowledge of nonequilibrium-dissociated boundary-layer behavior is also required in fundamental studies which seek to determine basic chemical kinetic and transport property data and to develop reliable devices for measurement of state properties in reacting gas flows (see, for example, [6–13] and the additional references cited in these papers).

Mathematically, this problem is a difficult one to solve for body shapes and gases of practical interest. This is because the dissociation–recombination reaction rates occurring in either simple diatomic gases or more complex gas mixtures such as dissociated air introduce highly complicated, nonlinear source terms into the governing specie and energy conservation equations. Moreover, except in the special case of stagnation point flow on a symmetric body [14], these source terms cause the flow to be [locally non-similar, thereby requiring the solution to a set of nonlinear partial differential equations. As a consequence of these difficulties, analytical solutions for realistic situations have been comparatively few. A number of early theoretical studies treated highly simplified physical models involving linearized chemical kinetics and idealized flow geometries [15–18]. However, with the exception of some recent approximate closed form solutions relating to certain aspects of nonequilibrium flat plate and stagnation point boundary layers in diatomic gases [7, 19–23], theoretical studies of the nonlinear

problem have been carried out on digital computers by a variety of numerical methods [14, 24–30]. Nevertheless, further investigations of an analytical nature for flow situations of practical interest will undoubtedly be useful at this stage of development to further illuminate the underlying physical behavior and to establish the functional relationships between nonequilibrium boundary-layer properties and the important thermochemical parameters.

Accordingly, this paper presents a study of analytical solutions to the laminar boundary-layer equations for highly nonequilibrium dissociated flows over non-ablating bodies with either a completely catalytic or perfectly non-catalytic surface. These solutions are obtained by a perturbation method wherein small local departures from a completely frozen boundary-layer flow are considered. This approach, while restricted to a small portion of the entire range of nonequilibrium-reaction effects between the extremes of completely frozen and completely equilibrium flow behavior, offers several significant advantages. First, it permits analytical solutions to be obtained, since the equations governing the nonequilibrium effects become linear. Second, the method need not place any restriction on the complexity of the reaction rates or the number of components involved, so that a realistic chemical model of either a diatomic or multicomponent gas such as air can be used. Third, the reaction rate effects need not be self-similar, so that a fairly wide class of flow configurations can be studied in a unified way. Also, it should be noted that the assumed situation of small gas phase reaction rates can in fact hold over a significant portion of sharp-nosed slender bodies at sufficiently low ambient densities. Moreover, in the general case, these nearly frozen flow solutions can be ery useful as starting solutions in carrying out nu nerical analyses at arbitrary reaction rate values.

The object of this paper is to exploit these advantages so as to obtain further insight to the behavior of nonequilibrium-dissociated, multicomponent boundary layers in both recombination-controlled and dissociation-controlled flow situations. Specific applications of the theory will be made to highly cooled stagnation point flows and hypersonic flows over sharp flat plates and slender cones. The accuracy of the binary mixture approximation for nonequilibrium-dissociated air [14], and the sensitivity of nonequilibrium boundary-layer solutions to both chemical kinetic data and transport properties are discussed in detail for these applications. In addition, the accuracy of the local similarity approximation and the use of nonequilibrium boundary-layer scaling laws will be examined for the plate and cone flows.

II. FORMULATION OF THE PROBLEM

A. *Assumptions*

Consider laminar boundary-layer flow of a reacting gas mixture around a two-dimensional or axially symmetric body. The body surface is regarded as impermeable and non-ablating. To simplify analysis of the nonequilibrium behavior, the following assumptions are made: (1) The gas is a four component mixture consisting of two molecular species with equal molecular weights and specific heats and two atomic species whose binary diffusion coefficients are equal and the same with respect to either of the molecular species. (2) Prandtl number Pr, Schmidt number Sc, and the density-viscosity product $\rho\mu$ are each constant across the boundary layer. (3) The average specific heat $\overline{c_P}$ of the mixture is constant across the boundary layer (i.e. the energy in molecular rotation and vibration is assumed negligible in comparison with the energy in translation and dissociation). (4) Thermal diffusion effects are negligible. (5) The velocity distribution across the boundary layer is locally self-similar and independent of the solutions to the energy and diffusion equations. (6) Pressure gradient effects on the energy equation can be neglected. (7) Low Reynolds number effects, such as vorticity interaction, induced pressure fields, curvature effects and slip phenomena at the surface, are neglected. (8) Any nonequilibrium reaction that may simultaneously occur in the inviscid flow at the edge of the boundary layer will have a negligible influence on the nonequilibrium effects within the boundary layer.

Assumption one obviously includes as an exact special case a dissociating diatomic gas. It also provides a realistic model of high temperature, nonequilibrium dissociated air in the

absence of ablation products or any *thermally significant* ionization as long as the influence of nitric oxide formation is small. To be sure, the formation of nitric oxide must be taken into account in calculating electron density profiles across nonequilibrium-dissociated air boundary layers on both sharp- or blunt-nosed hypervelocity aerodynamic bodies [5, 27, 30]. However, for the purpose of studying the thermally significant properties of highly cooled, recombination-dominated boundary layers, a four component mixture consisting of O_2, N_2, O, and N is sufficient because the energy of any NO present is usually negligible [27]. The effect of nitric oxide formation may not be as small in highly dissipative, dissociation rate-dominated boundary layers if there occur pronounced NO concentration overshoots analogous to those observed behind shock waves [31]. Assumption two tends to break down for highly dissociated gases because $\rho\mu$ and Sc are affected strongly by dissociation through the compressibility term in the thermal equation of state [32]. Nevertheless, assumptions one through four generally are acceptable engineering approximations in analyzing non-ablating, highly cooled dissociated air boundary layers on blunt bodies unless the finer details of the temperature and composition profiles are of interest [23, 26, 33–37]. However, as will be shown below, a more detailed consideration of the multicomponent mixture transport properties appears to be necessary for highly dissipative nonequilibrium boundary-layer flows around sharp-nosed slender bodies. With $\rho\mu = \text{constant}$, assumptions five and six are exact for supersonic flows over a wedge or cone; whereas for incompressible flow over wedges, assumption five is also exact, while six still remains a good good approximation because of the low velocities involved. Furthermore, with the exception of flows in adverse pressure gradients, these assumptions have been shown to be satisfactory approximations in solving the boundary layer energy and diffusion equations for the flow around sharp-nosed slender bodies and highly cooled blunt bodies in hypersonic flow [1, 26, 33–35, 38–40]. According to a theoretical study by Chung [41], the low Reynolds number phenomena neglected under assumption seven appear to be important only flow regimes where the boundary layer has already become completely frozen, at least for stagnation flows in atmospheric flight. However, this conclusion should be viewed with caution in the case of sharp-nosed, slender bodies, where the self-induced pressure field and fully viscous shock layer effects may have an important effect on the nonequilibrium relaxation behavior [20]. Finally, the neglect of nonequilibrium reaction effects in the inviscid flow compared to those within the boundary layer under assumption eight has been shown to be a satisfactory approximation except in the case of unsteady boundary layers developing in the slow, rapidly dissociating gas flow behind a strong shock in a shock tube [29, 42].

In connection with the foregoing assumptions, it should be emphasized that it it not intended here to consider all those aspects of the problem that can be important in a detailed calculation. For example, the effect of the multicomponent reaction rate terms in the presence of both oxygen and nitrogen atoms and molecules in nonequilibrium air will be studied in some detail even though NO has been neglected and a simple model of the multicomponent mixture transport properties has been assumed. To be sure, as noted above, the results of such a theory undoubtedly give an incomplete account of nonequilibrium air boundary layers around sharp-nosed slender bodies, and should be supplemented by consideration of the effects of NO-formation and a more accurate representation of the multicomponent transport properties. The aim of the present paper is thus to explore only certain parts of the problem which can be treated analytically and yet are essential ingredients in any more complete theory.

B. *Boundary-layer equations*

Let α_i denote the i-th specie mass fraction, where in the case of air, the four species O_2, O, N_2, and N are denoted by the indices $i = 1, 2, 3, 4$, respectively. Then by defining a stream function $\psi(\xi, \eta) = \sqrt{(2\xi)} f(\eta)$ such that

$$u/u_e = \partial f/\partial\eta \equiv f'(\eta),\dagger$$

† According to assumption six, $f(\eta)$ is regarded as a known function (e.g. the Blasius function in the case of supersonic wedge or cone flows).

employing the well-known similarity co-ordinate transformation [33, 34]

$$\xi \equiv \int_0^x C\rho_e \mu_e u_e r_B^{2\epsilon}\,\mathrm{d}x \qquad \left\{\begin{matrix}\epsilon = 0, \text{ two-dimensional}\\ \epsilon = 1, \text{ axisymmetric}\end{matrix}\right\} \quad (1)$$

$$\eta \equiv \frac{r_B^{\epsilon} u_e}{\sqrt{(2\xi)}} \int_0^y \rho\,\mathrm{d}y$$

(where $C = \rho\mu/\rho_e\mu_e$ is an appropriate constant), and introducing the variables $z_i = \alpha_i/\alpha_{i_e}$, $\theta = T/T_e$ and $\kappa = x\,\mathrm{d}\ln\xi/\mathrm{d}x$, the governing diffusion and energy equations for the boundary-layer flow of these four reacting species can be written under the above assumptions as follows:

$$Scf\frac{\partial z_i}{\partial\eta} + \frac{\partial^2 z_i}{\partial\eta^2} = \frac{2x\,Sc}{\kappa u_e}\left(\frac{\dot{w}_i}{\rho\alpha_{i_e}}\right) + 2\xi f'\,Sc\frac{\partial z_i}{\partial\xi} \qquad (i = 2, 4) \quad (2)$$

$$z_4\,\alpha_{4_e} + z_3\,\alpha_{3_e} = \text{constant} \simeq 0{\cdot}79 \quad (3)$$

$$Prf\frac{\partial\theta}{\partial\eta} + \frac{\partial^2\theta}{\partial\eta^2} + \frac{Pr\,u_e^2}{\overline{c_P}\,T_e}(f'')^2 = -\frac{2x\,Pr}{\kappa u_e}\sum_{i=2,4}\frac{H_{D_i}\dot{w}_i}{\rho} + 2\xi f'\,Pr\frac{\partial\theta}{\partial\eta} \quad (4)$$

where $H_{D_i} = h_{f_i}^0/\overline{c_P}\,T_e$ is the specific dissociation energy of the i-th atomic specie expressed as a fraction of the inviscid flow thermal energy ($h_{f_i}^0$ being zero for the molecules) and $\dot{w}_i$ is the net volumetric rate of i-th specie atom mass destruction due to chemical reaction as formulated below. In deriving equations (2) and (4), the streamwise composition derivatives in the inviscid flow have been neglected in accordance with assumption eight. Equation (3) expresses the fact that the total number of nitrogen atoms in the mixture, regardless of their chemical form, is invariant to chemical reaction, convection, or diffusion. As a result of this relation and the conditions $\sum\dot{w}_i = 0$ and $\sum\alpha_i = 1$, only two species conservation equations for the two respective atomic species are needed.

The boundary conditions to be imposed on the solution to equations (2) through (4) are as follows. At the edge of the boundary layer $\eta \to \infty$, $z_i(\xi, \infty) = \theta(\xi, \infty) = f'(\infty) = 1$. At the wall $\eta = 0$, $f(0) = f'(0) = 0$, $\theta(0, \xi) = \theta_w(\xi)$. Furthermore, since the present study is primarily concerned with the effects of nonequilibrium homogeneous reaction, only the two extreme cases for the effect of heterogeneous atom recombination on the body surface will be considered [43–45], namely either a perfectly catalytic wall [$z_{2,4}(\xi, 0) = 0$]† or a completely non-catalytic wall [$\partial z_{2,4}/\partial\eta(\xi, 0) = 0$]. Approximate analyses of the simultaneous effects of finite gas phase and surface recombination rates for highly cooled stagnation point boundary layers may be found, for example, in [7, 21, and 23]. Once the atom concentration and temperature distributions are known, the heat-transfer rate $\dot{q}_w$ to the body can be computed from

$$\frac{-Pr\,(\dot{q}_w/\overline{c_P}\,T_e)}{[(\kappa/2)\,C\rho_e\mu_e\,(u_e/x)]^{1/2}} \equiv Q_w = \frac{\partial\theta}{\partial\eta}(\xi, 0) + Le\sum_{i=2,4}\alpha_{i_e}\,H_{D_i}\frac{\partial z_i}{\partial\eta}(0, \xi) \quad (5)$$

where $Le = Pr/Sc$ is the Lewis number. It is observed that only heat conduction contributes to the heat transfer when the wall is perfectly non-catalytic or when the gas is undissociated ($\alpha_2 = \alpha_4 = 0$).

C. *Reaction rates*

For the high temperature air model assumed, the rate chemistry in the boundary layer consists of the following two independent dissociation–recombination reactions for oxygen and nitrogen, respectively:

$$N_1 + N_x \underset{k_{R_2}}{\overset{k_{D_2}}{\rightleftharpoons}} 2N_2 + N_x \quad (6a)$$

$$N_3 + N_x \underset{k_{R_4}}{\overset{k_{D_4}}{\rightleftharpoons}} 2N_4 + N_x \quad (6b)$$

where N_i denotes the number of moles of the i-th species and the third body acting as the catalyst

† The wall temperature is assumed to be low enough ($\lesssim$2000°K) that the equilibrium atom concentrations at the gas/solid interface are zero.

for recombination (subscript x) may be any one of the four species present. Let the equilibrium constants and recombination rates be of the general form

$$\frac{k_{D_i}}{k_{R_i}} = \frac{Np_0}{p}\left(\frac{T}{T_{R_1}}\right)^{s_i} \exp\left(A_i - \frac{T_{D_i}}{T}\right) = \frac{Np_{D_i}}{p}\left(\frac{T}{T_e}\right)^{s_i} \exp\left(-\frac{T_{D_i}}{T}\right) \tag{7}$$

and $k_{R_i} = k'_{R_{ix}}(T/T_{R_2})^{\omega_i}$, respectively [31, 46–48], where A_i, s_i, and ω_i are constants, p_0 is atmospheric pressure, T_{R_1} and T_{R_2} are constant reference temperatures, $N = \sum N_i$,

$$p_{D_i} = p_0 (T_e/T_{R_1})^{s_i} \exp A_i$$

is a characteristic dissociation pressure of the molecules, and $T_{D_i} = 2h^0_{f_i} m_i/\mathscr{R}_u$ is the molecular dissociation temperature. Then application of the laws of phenomenological rate kinetics [49] and the thermal equation of state $p = (\mathscr{R}_u/m_m)\, T(1 + \alpha_2 + \alpha_4)\rho$ for the present problem yields the following net reaction rates:

$$\frac{\dot{w}_2}{\rho} = -\frac{\dot{w}_1}{\rho} = 2\left(\sum_x k'_{R_{2x}}\frac{N_x}{N}\right)\left(\frac{p_e}{\mathscr{R}_u T}\right)^2 \left(\frac{T}{T_{R_2}}\right)^{\omega_2} \times \left[\frac{\alpha_2^2}{1 + \alpha_2 + \alpha_4} - \left(\frac{1 - \alpha_2 - \alpha_3 - \alpha_4}{4}\right)\frac{p_{D_2}}{p_e}\theta^{s_2} \exp\left(\frac{\theta_{D_2}}{\theta}\right)\right] \tag{8a}$$

$$\frac{\dot{w}_4}{\rho} = -\frac{\dot{w}_3}{\rho} = 2\left(\sum_x k'_{R_{4x}}\frac{N_x}{N}\right) \left(\frac{p_e}{\mathscr{R}_u T}\right)^2 \left(\frac{T}{T_{R_2}}\right)^{\omega_4} \left[\frac{\alpha_4^2}{1 + \alpha_2 + \alpha_4} - \frac{\alpha_3}{4}\frac{p_{D_4}}{p_e}\theta^{s_4} \exp\left(-\frac{\theta_{D_4}}{\theta}\right)\right] \tag{8b}$$

where the square bracketed quantities on the right-hand sides have the important property of vanishing identically at equilibrium. Obviously, equations (8) also apply in the special case of a pure diatomic dissociating gas composed of atoms (subscript a) and molecules (subscript m) by setting, for example, $\alpha_3 = \alpha_4 = 0$ and $\alpha_2 = \alpha_a = 1 - \alpha_1 = 1 - \alpha_m$. It is noted that the net recombination rate coefficient for either atomic specie is a molar-average of the coefficients $k'_{R_{ix}}$ pertaining to each possible catalyst specie x. This is because the catalytic efficiencies of O, N, O_2, and N_2 with respect to a given atom are generally not the same [31, 48]. To simplify the subsequent analysis, appropriate constant values will be assumed for these two averaged coefficients, since the effect of their variation across the boundary layer would appear to be small compared to the variation of remaining composition and temperature-dependent terms in equations (8). Moreover, since available experiment [47, 48] and theory [50] indicate that the recombination rate exponent ω_i is essentially the same for O, N and most other diatomic gases ($\omega_i \simeq 0$ to $-1{\cdot}5$), it is henceforth assumed that $\omega_2 = \omega_4 = \omega$.

Introducing the previously defined non-dimensional variables into equations (8) and using assumption eight by setting $\dot{w}_{i_e} = 0$, the chemical source terms in equations (2) and (4) can be written

$$\frac{2x\, Sc\, \dot{w}_i}{\kappa u_e\, \rho a_{i_e}} = \Gamma \lambda_i\, G_i \qquad (i = 2, 4) \tag{9}$$

where

$$G_2 \equiv \theta^{\omega-2}\left\{\frac{(1 + \alpha_{2_e} + \alpha_{4_e})\, z_2^2}{1 + \alpha_{2_e} z_2 + \alpha_{4_e} z_4} - \left(\frac{0{\cdot}21 - \alpha_{2_e} z_2}{0{\cdot}21 - \alpha_{2_e}}\right)\theta^{s_2} \exp\left[-\frac{\theta_{D_2}}{\theta}(1 - \theta)\right]\right\} \tag{10a}$$

$$G_4 \equiv \theta^{\omega-2}\left\{\frac{(1 + \alpha_{2_e} + \alpha_{4_e})\, z_4^2}{1 + \alpha_{2_e} z_2 + \alpha_{4_e} z_4} - \left(\frac{0{\cdot}79 - \alpha_{4_e} z_4}{0{\cdot}79 - \alpha_{4_e}}\right)\theta^{s_2} \exp\left[-\frac{\theta_{D_4}}{\theta}(1 - \theta)\right]\right\} \tag{10b}$$

$$\lambda_2 \equiv \left(\sum_x \frac{k'_{R_{2x}}}{k'_{R_{22}}}\frac{N_x}{N}\right)\frac{\alpha_{2_e}}{1 + \alpha_{2_e} + \alpha_{4_e}} = \bar{\lambda}_2 \frac{\alpha_{2_e}}{1 + \alpha_{2_e} + \alpha_{4_e}} \tag{11a}$$

$$\lambda_4 \equiv \left(\sum_x \frac{k'_{R_{4x}}}{k'_{R_{22}}}\frac{N_x}{N}\right)\frac{\alpha_{4_e}}{1 + \alpha_{2_e} + \alpha_{4_e}} = \bar{\lambda}_4 \frac{\alpha_{4_e}}{1 + \alpha_{2_e} + \alpha_{4_e}} \tag{11b}$$

Here,

$$\Gamma = \frac{8\, k'_{R_{22}} (T_e/T_{R_2})^{\omega-2} (p_e/\mathscr{R}_u)^2\, x\, Sc}{\kappa u_e T_{R_2}^2} \qquad (12)$$

is a characteristic (flow-time/recombination-time) ratio for the boundary layer similar to that defined by Fay and Riddell [14]. When $\Gamma = 0$, the flow is chemically frozen with the reaction terms in equations (2) and (4) neglected (although the G_i are not zero), whereas if $\Gamma \to \infty$, the flow tends toward an equilibrium state throughout the boundary layer defined by

$$G_2(\eta) = G_4(\eta) = 0.$$

Since Γ is directly proportional to x and also depends on the local inviscid flow pressure, temperature, and velocity as well as the body shape, the degree of departure from chemical equilibrium within the boundary layer can vary appreciably along the body. Therefore, the effects of nonequilibrium reaction in the boundary layer are generally non-similar (depending on ξ as well as η). Only in the special case of stagnation point flow on a symmetric body ($u_e \sim x$; p_e, T_e, κ = constant) is Γ independent of x and the nonequilibrium boundary layer therefore exactly self-similar [14].

D. *The binary mixture approximation for nonequilibrium air*

In their analysis of nonequilibrium boundary-layer flow of dissociated air at a stagnation point, Fay and Riddell [14] employed a simplified representation of the net dissociation–recombination reaction rate terms for the mixture wherein air was treated as an effective diatomic gas composed of "air molecules" and "air atoms". Since one of the objectives of this paper is to evaluate the importance of the multicomponent gas reaction rate terms in analyses of nonequilibrium air boundary layers, a description of this binary approximation is appropriate at this point.

Consider the present four-component gas mixture from the standpoint of determining the distribution of the total atom mass fraction $\alpha = \alpha_2 + \alpha_4 = \alpha_{2_e} z_2 + \alpha_{4_e} z_4$. Introducing the variable $Z = \alpha/\alpha_e$ and using equations (2), the equation governing the change in α across a nonequilibrium boundary layer can be written as follows:

$$Sc\, f \frac{\partial Z}{\partial \eta} + \frac{\partial^2 Z}{\partial \eta^2} - 2\xi f'\, Sc \frac{\partial Z}{\partial \xi} = \frac{2x\, Sc}{\kappa u_e}\left(\frac{\dot{w}_2 + \dot{w}_4}{\rho a_e}\right) \equiv \frac{2x\, Sc}{\kappa u_e}\left(\frac{\dot{w}_Z}{\rho a_e}\right) \qquad (13)$$

Now the binary mixture model for dissociating air consists of approximating the total atom rate on the right side of (13) by the net recombination–dissociation rate that would exist in a pure diatomic gas with a relative atom mass fraction Z, as follows:

$$\frac{2x\, Sc}{\kappa u_e}\frac{\dot{w}_Z}{\rho a_e} \simeq \lambda_2 \Gamma \frac{\alpha_e}{1+\alpha_e}\theta^{\omega-2}\left\{\left(\frac{1+\alpha_e}{1+\alpha_e Z}\right) Z^2 - \left(\frac{1-\alpha_e Z}{1-\alpha_e}\right)\theta^{s_2} \exp\left[-\frac{\theta_{D_2}}{\theta}(1-\theta)\right]\right\} \qquad (14)$$

Consistent with this approximation, one may also employ a corresponding approximation for the reaction rate-dissociation energy product summation on the right side of the energy equation (4). Thus, following [14], this summation is represented by the following equivalent binary form:

$$\sum_i H_{D_i}\frac{\dot{w}_i}{\rho} \simeq \left(\sum_i \frac{\alpha_{i_e}}{\alpha_e} H_{D_i}\right)\frac{\dot{w}_Z}{\rho} \equiv \bar{H}_D \frac{\dot{w}_Z}{\rho} \qquad (15)$$

that is, the sum of the products of the individual atom reaction rates and dissociation energies is approximated by the product of an averaged dissociation energy $\bar{H}_D$ and the net atom reaction rate based on the binary gas model. Correspondingly, the diffusion heat flux contribution to the surface heat transfer can be written

$$\sum_i H_{D_i}\alpha_i \frac{\partial z_i}{\partial \eta}(\xi, 0) \simeq \bar{H}_D\, \alpha_e \frac{\partial Z}{\partial \eta}(\xi, 0) \qquad (16)$$

Approximations (14)–(16) do not follow from a development of the exact expressions but are based on intuitive physical reasoning following the idea of an equivalent binary mixture. Obviously, a very convenient formulation of the problem is thereby obtained, since the nonequilibrium effects on the composition field

throughout the boundary layer are expressed solely in terms of the *total* atom mass fraction The error incurred by using these approximations will be examined below.

III. SOLUTION FOR NEARLY FROZEN NONEQUILIBRIUM FLOWS

A. *Perturbation method*

The mathematical difficulties connected with the highly nonlinear reaction terms in equations (2) and (4) naturally invite a more restricted approach wherein attention is confined to small departures from a completely frozen flow ($\Gamma(\xi) \ll 1$). One thereby trades the ability of treating the complete range of nonequilibrium reaction effects for the advantages of dealing with linear differential equations. Accordingly, we expand each of the dependent variables about its local frozen value as follows:

$$\left.\begin{aligned} z_i(\xi,\eta) &= z_{F_i}(\eta) + \Gamma(\xi)\, z_{I_i}(\eta) \\ &\quad + \Gamma^2(\xi)\, z_{II_i}(\eta) + \ldots \quad (i = 2, 4) \\ \theta(\xi,\eta) &= \theta_F(\xi,\eta) + \Gamma(\xi)\,\theta_I(\eta) \\ &\quad + \Gamma^2(\xi)\,\theta_{II}(\eta) + \ldots \end{aligned}\right\} \quad (17)$$

where subscript F denotes the frozen flow solution, subscript I denotes the first-order perturbations due to nonequilibrium reaction, etc. On substituting these series into equations (2), (4) and (9), equating to zero the net coefficient of each power of Γ, and confining attention to first-order effects,† one obtains the following two sets of equations governing the zeroth-order (frozen) flow and first-order nonequilibrium perturbations, respectively:

$$Scf z'_{F_i} + z''_{F_i} = 0 \quad (i = 2, 4) \qquad (18)$$

$$Prf\frac{\partial\theta_F}{\partial\eta} + \frac{\partial^2\theta_F}{\partial\eta^2} + \frac{Pr\,u_e^2}{c_P T_e}(f'')^2 = 2\,Pr\,\xi f'\frac{\partial\theta_F}{\partial\xi} \qquad (19)$$

and

$$Sc\,fz'_{I_i} + z''_{I_i} - 2\left(\frac{\xi}{\Gamma}\frac{d\Gamma}{d\xi}\right) Scf' z_{I_i} = \lambda_i G_{F_i}(\eta) \quad (i = 2, 4) \qquad (20)$$

† A detailed treatment of second order effects ($\sim\Gamma^2$), which entails a far more complicated and laborious analysis, may be found in [35].

$$Prf\theta'_I + \theta''_I - 2\left(\frac{\xi}{\Gamma}\frac{d\Gamma}{d\xi}\right) Prf'\theta_I = -Le\sum_{i=2,4}\alpha_{i_e} H_{D_i}\lambda_i G_{F_i}(\eta) \qquad (21)$$

The corresponding boundary conditions for $i = 2, 4$ are $z_{F_i}(\infty) = \theta_F(\xi, \infty) = 1$, $z_{I_i}(\infty) = \theta_I(\infty) = 0$, $\theta_F(\xi, 0) = \theta_w(\xi)$, $\theta_I(0) = 0$ and either $z_{F_i}(0) = z_{I_i}(0) = 0$ for a catalytic wall or $z'_{F_i}(0) = z'_{I_i}(0) = 0$ for a non-catalytic wall. The first-order nonequilibrium heat-transfer rate Q_w becomes

$$\left.\begin{aligned} Q_w &= Q_{w_F} + \Gamma Q_{w_I} \\ &= \frac{\partial\theta_F}{\partial\eta}(\xi, 0) + Le\sum_{i=2,4}\alpha_{i_e} H_{D_i} z'_i(0) \\ &\quad + \Gamma[\theta'_I(0) + Le\sum_{i=2,4}\alpha_{i_e} H_{D_i} z'_{I_i}(0)] \end{aligned}\right\} \quad (22)$$

B. *Frozen solution*

The diffusion equations (18) for the two atomic species are ordinary differential equations because α_{ie} and the wall boundary conditions are assumed independent of x. Their solution [43] in terms of the known stream function $f(\eta)$ is

$$\left.\begin{aligned} z_{F_i}(\eta) = Z_F(\eta) &= \frac{\int_0^\eta \exp\left(-Sc\int_0^\eta f\,d\eta\right) d\eta}{\int_0^\infty \exp\left(-Sc\int_0^\eta f\,d\eta\right) d\eta} \\ &\equiv \frac{I(\eta, Sc)}{I(\infty, Sc)}, \quad \text{catalytic wall} \\ &\qquad\qquad (i = 2, 4) \\ &= 1, \quad \text{non-catalytic wall} \end{aligned}\right\} \quad (23)$$

In the important special case of a negligible pressure gradient, where f is the Blasius function $f_B(\eta)$ satisfying $f_B f''_B + f'''_B = 0$, one has $I(\eta, Sc) = [f''_B(0)]^{-Sc}\int_0^\eta [f''_B(\eta)]^{Sc}\,d\eta$ with $f''_B(0) = 0{\cdot}47$ and $I(\infty, Sc) \simeq (0{\cdot}47\,Sc^{1/3})^{-1}$.

The energy equation (19) is a partial differential equation because θ_F will not be self-similar in the general case where either T_w, T_e, or u_e vary arbitrarily along the body. Various exact and approximate solutions for such cases are available in the literature and need not be discussed in detail here. It is noted, however, that in the special case of uniform surface

temperature and negligible pressure gradient, the following self-similar solution to (19) is obtained:

$$\theta_F(\eta) = \theta_w + (1 - \theta_w)\frac{I(\eta, Pr)}{I(\infty, Pr)} + \left(\frac{u_e^2}{2\overline{c_P}\,T_e}\right)\left[\frac{I(\eta, Pr)}{I(\infty, Pr)}\theta_P(\infty, Pr) - \theta_P(\eta, Pr)\right] \quad (24)$$

where

$$\theta_P(\eta, Pr) \equiv 2\,Pr\int_0^\eta [f''(\eta)]^{Pr}\left\{\int_0^\eta [f''(\eta)]^{2-Pr}\,d\eta\right\}d\eta;\ \theta_P(\infty, Pr) \simeq \sqrt{(Pr)} \quad (25)$$

The last term in equation (24) represents the effect of viscous dissipation heating (negligible for incompressible flows). The functions $I(\eta)$ and $\theta_P(\eta)$ based on the Blasius function are well tabulated in the literature on boundary-layer theory.

Substituting (23) through (25) into (22), the frozen boundary-layer heat transfer can be written

$$\left.\begin{aligned} Q_{w_F} &= [I(\infty, Pr)]^{-1}\left[1 - \theta_w + \theta_P(\infty, Pr)\frac{u_e^2}{2\overline{c_P}\,T_e}\right. \\ &\left. + J\,Le\frac{I(\infty, Pr)}{I(\infty, Sc)}(\alpha_{2_e}H_{D_2} + \alpha_{4_e}H_{D_4})\right] \\ &\simeq 0{\cdot}47\,Pr^{1/3}\left[1 - \theta_w + \frac{\sqrt{(Pr)}\,u_e^2}{2\overline{c_P}\,T_e}\right. \\ &\left. + J\,Le^{2/3}(\alpha_{2_e}H_{D_2} + \alpha_{4_e}H_{D_4})\right] \end{aligned}\right\} \quad (26)$$

where $J = 1$ for a catalytic wall and $J = 0$ for a perfectly non-catalytic wall. This relation clearly shows the well-known result that a substantial reduction of heat transfer from a frozen, dissociated boundary layer can be obtained by maintaining a very low surface catalycity and thus preventing release of the heat of recombination to the body. This is true regardless of the Lewis number.

Based on solutions (23) and (24), some typical distributions of the frozen reaction rate function $G_{F_2}(\eta)$ [which is representative of both the non-homogeneous "forcing functions" $G_{F_i}(\eta)$ appearing in the first-order perturbation equations] are plotted in Figs. 1(a)–1(c) for either a catalytic or non-catalytic wall. Consider the case of highly cooled, low velocity flows involving small or negligible viscous dissipation [Fig. 1(a)], such as in the stagnation region of a blunt body in hypersonic flow. Here, gas phase recombination ($\sim Z_F^2$) near the wall is the controlling reaction rate within the boundary layer so that the $G_{F_i}(\eta)$ are predominantly positive. As a result, the magnitude and distribution of the $G_{F_i}(\eta)$ near the wall are significantly affected by the surface catalycity due to the influence of the species boundary conditions on the recombination term. However, these functions are seen to be relatively insensitive to the exponential dissociation rate term (θ_{D_i}) except in the outer portion of the boundary layer. Consequently, the approximation $G_{F_2} = G_{F_4}$ holds very well throughout the inner portion of the boundary layer. Consider now the case of locally high speed flows where viscous dissipation heating is large [Fig. 1(c)], such as those around a slender wedge or cone in a cold, hypervelocity gas stream. Here, the functions $G_{F_i}(\eta)$ are dominated by the exponential dissociation rate term and hence predominantly negative. The dissociation rate has a pronounced maximum at a location $\eta = \eta^*$ corresponding to the maximum frozen flow temperature. In contrast to the aforementioned low speed, recombination-controlled flows, the functions $G_{F_i}(\eta)$ are relatively unaffected by the surface catalycity when T_w is well below the recovery temperature. Furthermore, the $G_{F_i}(\eta)$ are now very sensitive to the parameter θ_{D_i} so that G_{F_2} and G_{F_4} can differ considerably from each other in the vicinity of the maximum reaction rate.

C. *First-order solution*

The linear, non-homogeneous equations (20) and (21) are readily solved by standard mathematical methods and involve quadratures of the frozen reaction rate distribution functions. These are ordinary differential equations because the perturbation distribution functions $z_{I_i}(\eta)$

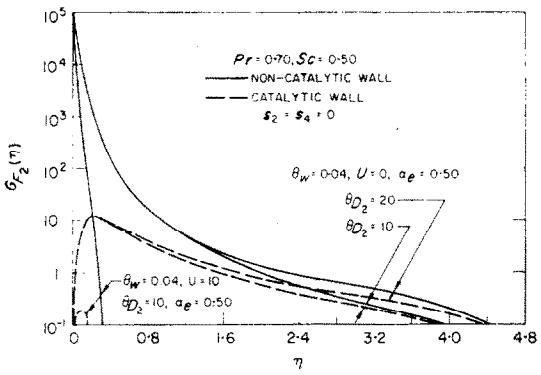

(a) HIGHLY COOLED, NON-DISSIPATIVE RECOMBINATION RATE CONTROLLED FLOWS

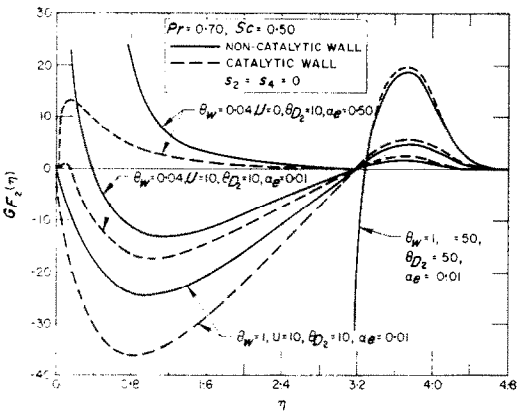

(b) HIGHLY COOLED DISSIPATIVE FLOWS

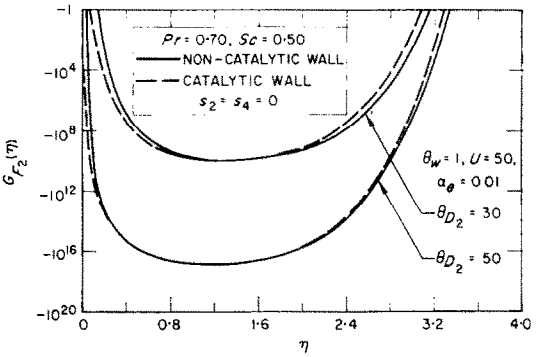

(c) HIGHLY DISSIPATIVE DISSOCIATION RATE CONTROLLED FLOWS

FIG. 1. Reaction rate distributions.

and $\theta_I(\eta)$ were taken to be self-similar in writing the series solutions (17). The non-similar effect of chemical reaction therefore resides entirely in the variation of $\Gamma(\xi)$ along the body. To be consistent with this assumption, both θ_{D_i} and the parameter $Q \equiv \xi[(d\Gamma/d\xi)/\Gamma]$ must be constant, so that $T_e = \text{constant}$ and $\Gamma \sim \xi^Q$ where Q is an arbitrary constant. These conditions are realized, for example, in supersonic flows over wedges or cones [$\xi \sim x^{2\epsilon+1}(2\epsilon + 1)^{-1} \sin^{2\epsilon}\delta$, $\Gamma \sim x$, $Q = \kappa^{-1} = (2\epsilon + 1)^{-1}$; $\delta =$ wedge or cone semi-angle], stagnation point flow on a blunt body in supersonic flow [$\xi \sim x^{2(1+\epsilon)}/2(1 + \epsilon)$, $Q = 0$, $\kappa = 2(1 + \epsilon)$] and for incompressible flow over wedges [$u_e \sim x^M$, $\delta = M\pi/(1 + M)$, $\xi \sim x^{M+1}/(M + 1)$. $0 \leq 1 \leq M$, $Q = (1 - M)/1 + M)$, $\kappa = 1 + M$†].

Equation (20) is solved in terms of the solution $\mathbf{s}(\eta, Q, Sc)$ to the associated homogeneous equation

$$Sc\, f\, \mathbf{s}' + \mathbf{s}'' - 2Q\, Sc\, f'\, \mathbf{s} = 0 \qquad (27)$$

with $\mathbf{s}(0) = 1$, $\mathbf{s}'(0) = 0$. This solution is unique for $Q > -1/2$ and is readily obtained by a straightforward numerical integration of equation (27) using Milne's method; typical results based on the Blasius function are plotted as a function of Sc and Q in Fig. 2. The full solutions

† Here, since ρ_e and T_e can be assumed constant, the thermal equation of state and equation (12) yield $\Gamma \sim x/u_e$.

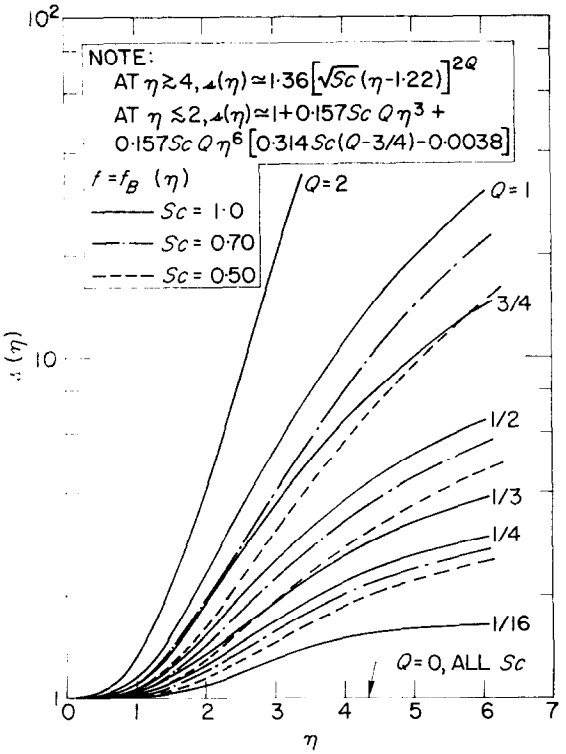

FIG. 2. The function $s(\eta)$.

to (20) for either a catalytic or non-catalytic surface can then be written [51]

$$\left.\begin{aligned} z_{I_i}(\eta) = & \\ & -\lambda_i \left\{ \left[1 - J + J \cdot \frac{I_s(\eta)}{I_s(\infty)} \right] \right. \\ & \left. \mathscr{I}_i(\infty, Sc) - \mathscr{I}_i(\eta, Sc) \right\} \cdot s(\eta, Sc) \\ & z'_{I_i}(0) = -J\lambda_i \mathscr{I}_i(\infty, Sc)/[1 - \\ & \quad J + J \cdot I_s(\infty)] \\ & z_{I_i}(0) = -(1 - \\ & \quad J)\, \lambda_i \mathscr{I}_i(\infty, Sc) \end{aligned}\right\} (i = 2, 4) \quad (28)$$

where

$$I_s(\eta, Sc) \equiv \int_0^\eta \frac{\exp\left(-Sc \int_0^\eta f\, d\eta\right)}{s^2(\eta, Sc, Q)}\, d\eta \quad (29)$$

$$\mathscr{I}_i(\eta, Sc) \equiv \int_0^\eta \frac{\exp\left(-Sc \int_0^\eta f\, d\eta\right)}{s^2(\eta, Sc)} \left[\int_0^\eta s(\eta, Sc) \exp\left(+Sc \int_0^\eta f\, d\eta\right) G_{F_i}(\eta)\, d\eta \right] d\eta \quad (30a)$$

$$= I_s(\eta, Sc) \int_0^\eta s(\eta, Sc) \exp\left(Sc \int_0^\eta f\, d\eta\right) G_{F_i}(\eta)\, d\eta - \int_0^\eta I_s(\eta, Sc)\, s(\eta, Sc) \exp\left(Sc \int_0^\eta f\, d\eta\right) G_{F_i}(\eta)\, d\eta \quad (30b)$$

The function $I_s(\eta, Sc)$ based on $f_B(\eta)$ is plotted in Fig. 3 for various values of Q. It should be emphasized that the reaction rate integrals (30b) for a catalytic or non-catalytic wall, respectively, will differ considerably in the case of recombination rate-controlled flows as is evident from Fig. 1(a). A comprehensive parametric study of this integral has been made over a wide range of the parameters Q, α_{i_e}, Sc, θ_{D_i}, ω and U for both catalytic and non-catalytic walls. A detailed description of these results is

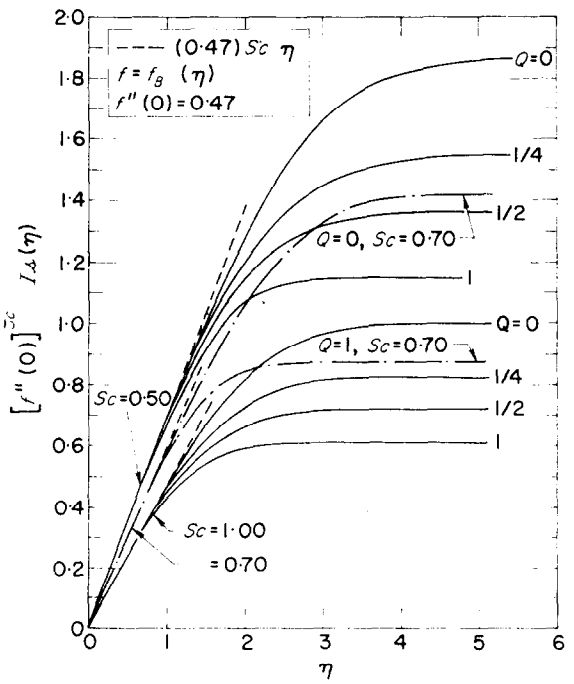

FIG. 3. The function $I_s(\eta)$.

given in reference 52 but is not presented here due to space limitations.

In connection with the foregoing solution, it is of interest to note a closed-form approximation for $\mathscr{I}_i(\infty)$ suggested by Rae [19] for highly dissipative flows where the exponential dissociation term in $G_{F_i}(\eta)$ is the dominant contribution and very large. Here, if $\theta_{D_i} \gg 1$, $f''(\eta^*) > 0$ and the recombination rate is neglected, the method of steepest descent [53] can be used to evaluate the integral $\mathscr{I}_i(\infty)$ from (30b) with the following result:

$$\mathscr{I}_i(\infty) \simeq \mathfrak{s}(\eta^*) \exp\left(Sc \int_0^{\eta^*} f\,\mathrm{d}\eta\right) [I_s(\infty) - I_s(\eta^*)] \sqrt{(\pi)} \left[\frac{1 + \operatorname{erf}(\eta^* \beta_i^*)}{2\beta_i^*}\right] G_{F_i}(\eta^*) \quad (31)$$

where $\beta_i^* = [(\theta_{D_i}/2)\ (1/\theta_F)''_{\eta^*}]^{1/2}$ and η^* here refers to the position of the frozen flow temperature maximum $[\theta'_F(\eta^*) \equiv 0]$. For constant wall temperature and negligible pressure gradient, equation (24) yields the following relation to determine η^* when the Prandtl number is near unity:

$$f'_B(\eta^*) \simeq \frac{1}{2}\left[1 + \frac{(1 - \theta_w)}{\sqrt{(Pr)}} \left(\frac{2\overline{c_P}\ T_e}{u_e^2}\right)\right] \quad (32)$$

which in turn gives

$$\beta_i^* \simeq f''_B(\eta^*)\ \theta_F^{-1}(\eta^*) \sqrt{\left(\frac{\theta_{D_i}}{2} \sqrt{(Pr)} \frac{u_e^2}{\overline{c_P}\ T_e}\right)} \quad (33)$$

Approximation (31) may be thought of as the product of the maximum reaction rate $G_{F_i}(\eta^*)$ and a form factor that accounts for the integrated effect of reaction across the entire boundary layer as modified by the influence of convection and diffusion. Correspondingly, the steepest descent method also gives $\mathscr{I}_i(\eta^*) \simeq 0$, which yields from equation (28):

$$z_{I_i}(\eta^*) \simeq \mathfrak{s}(\eta^*)\ \lambda_i \left[1 - J + J \cdot \frac{I_s(\eta^*)}{I_s(\infty)}\right] [-\mathscr{I}_i(\infty)] \quad (34)$$

Now, as shown in reference 52, the exact values of $\mathscr{I}_i(\eta^*)$ for wall temperatures well below recovery temperature are equal to $0{\cdot}2\,\mathscr{I}_i(\infty) - 0{\cdot}3\,\mathscr{I}_i(\infty)$, so that $\mathscr{I}_i(\eta^*) \simeq 0$ in itself is a poor approximation. However, since it is also found that the corresponding approximation (31) underestimates $\mathscr{I}_i(\infty)$ by about thirty per cent, equation (34) shows that the two errors nearly cancel each other in determining the $z_{I_i}(\eta^*)$.

Turning to the first-order energy equation (21), it can be seen that the solution for $\theta_I(\eta)$ is of the same form as the atom concentration perturbation for a catalytic wall when Sc is replaced by Pr in the functions $\mathfrak{s}(\eta, Sc, Q)$ and $\exp\left(\pm Sc \int_0^{\eta} f\,\mathrm{d}\eta\right)$. Thus, one readily finds

$$\left.\begin{aligned} \theta_I(\eta) &= Le \sum_{i=2,4} a_{i_e}\ \lambda_i\ H_{D_i} \left[\frac{I_s(\eta, Pr)}{I_s(\infty, Pr)} \bar{\mathscr{I}}_i(\infty, Pr) - \bar{\mathscr{I}}_i(\eta, Pr)\right] \mathfrak{s}(\eta, Pr, Q) \\ \theta'_I(0) &= Le \sum_{i=2,4} a_{i_e}\ \lambda_i\ H_{D_i} \frac{\bar{\mathscr{I}}_i(\infty, Pr)}{I_s(\infty, Pr)} \end{aligned}\right\} \quad (35a)$$

where

$$\bar{\mathscr{I}}_i(\eta, Pr) = \int_0^{\eta} \frac{\exp\left(-Pr \int_0^{\eta} f\,\mathrm{d}\eta\right)}{\mathfrak{s}^2(\eta, Pr)} \left[\int_0^{\eta} \mathfrak{s}(\eta, Pr) \exp\left(Pr \int_0^{\eta} f\,\mathrm{d}\eta\right) G_{F_i}(\eta)\,\mathrm{d}\eta\right] \mathrm{d}\eta \quad (35b)$$

Then, substituting solutions (28) and (35) into equation (22), the first-order heat-transfer perturbation due to nonequilibrium reaction becomes

$$Q_{w_I} = Le \sum_{i=2,4} a_{i_e}\ \lambda_i\ H_{D_i} \left[\frac{\mathscr{I}_i(\infty, Pr)}{I_s(\infty, Pr)} - J \frac{\mathscr{I}_i(\infty, Sc)}{I_s(\infty, Sc)}\right] \quad (36)$$

For a non-catalytic wall ($J = 0$), this heat-transfer perturbation is due entirely to the effect of gas phase reaction on the surface temperature gradient at the wall. From Fig. 1 and equation (30a) it is seen to be positive for recombination-controlled reaction in the boundary layer and negative for dissocation-controlled flows. These conclusions are essentially independent of the Lewis number. For a completely catalytic wall ($J = 1$), Q_{w_I} is much smaller since the effect of chemical reaction on the temperature gradient and diffusion heat

flux, respectively, is nearly the same but opposite in sign. Moreover, in this case, the sign of Q_{w_I} depends strongly on whether the Lewis number is greater or less than unity, since it is seen that $(Q_{w_I})_{J=1} = 0$ for $Le = 1 (\mathscr{I}_i = \overline{\mathscr{I}_i})$ The vanishing effect of gas phase reaction on heat transfer to a completely catalytic wall for $Le = 1$ is a well-known result [14, 33, 34], and follows from the fact that the total enthalpy distribution *throughout* the boundary layer for $Le = 1$ is unaffected by reaction. This can be inferred directly from equations (28) and (35) by observing that the total enthalpy perturbation $\theta_I(\eta) + \sum a_{ie} H_{D_i} z_{I_i}$ is zero when $Le = 1$ and $z_{I_i}(0) = 0$.

IV. APPLICATIONS OF THE THEORY

From the present theory, the first-order effects of nonequilibrium dissociation–recombination reaction can be readily calculated for a variety of flow conditions and body shapes. Among the possible applications, those involving stagnation point flow on a blunt body and hypersonic flow around either a flat plate or cone are of particular interest and will be considered in the remainder of this paper.

A. *Highly cooled stagnation point flow*

Aside from its obvious practical importance in missile technology, this case is also of interest here because comparison can be made with Fay and Riddell's numerical results for the complete nonequilibrium flow regime based on the binary mixture model for air [14]. Here, the controlling nonequilibrium reaction is the atom recombination rate in the gas near the cold wall. Typical total atom concentration and temperature profiles across the stagnation point boundary layer in air on an axisymmetric body ($Q = 0$, $\kappa = 4$) according to the present theory are plotted as a function of Γ in Figs. 4(a) and 4(b). These curves illustrate how a departure from completely frozen flow toward equilibrium reduces the atom concentration near the wall (and raises the temperature) due to the growing recombination rate near the wall. The corresponding behavior of the total atom concentration (or concentration gradient), temperature gradient and heat transfer at both a non-catalytic and a catalytic wall is shown in Figs. 5(a) and 5(b), respectively. In these figures, the results of the present theory for both the four-component mixture and the binary gas model are shown together with the corresponding numerical results of [14] for the latter model. The present theory for the binary model is seen to agree reasonably well with the nearly frozen results of [14] in the non-catalytic

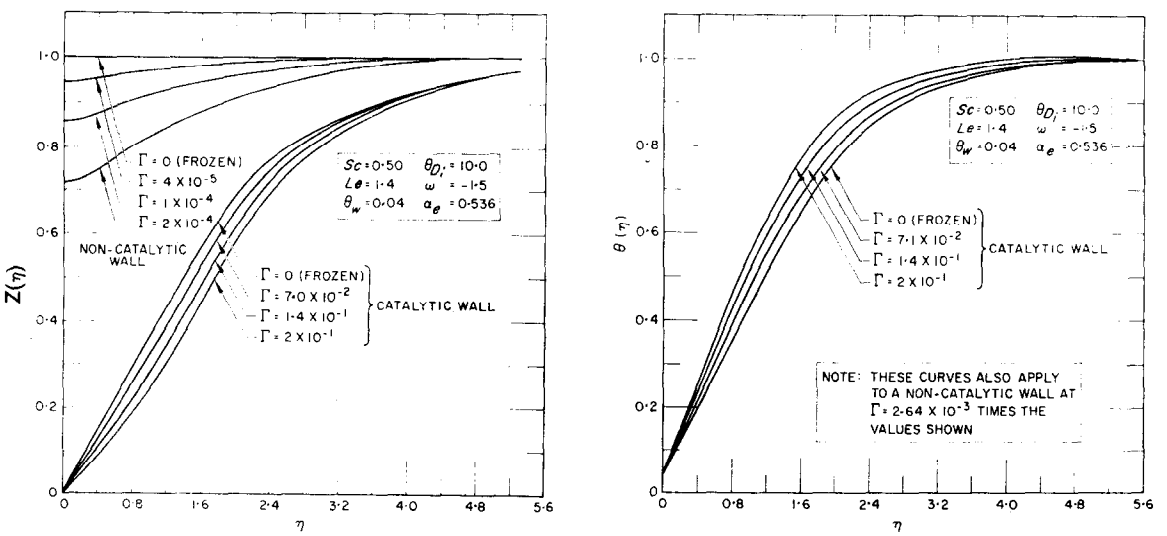

(a) TOTAL ATOM CONCENTRATION (b) TEMPERATURE

FIG. 4. State profiles across a highly cooled, nonequilibrium stagnation point boundary layer.

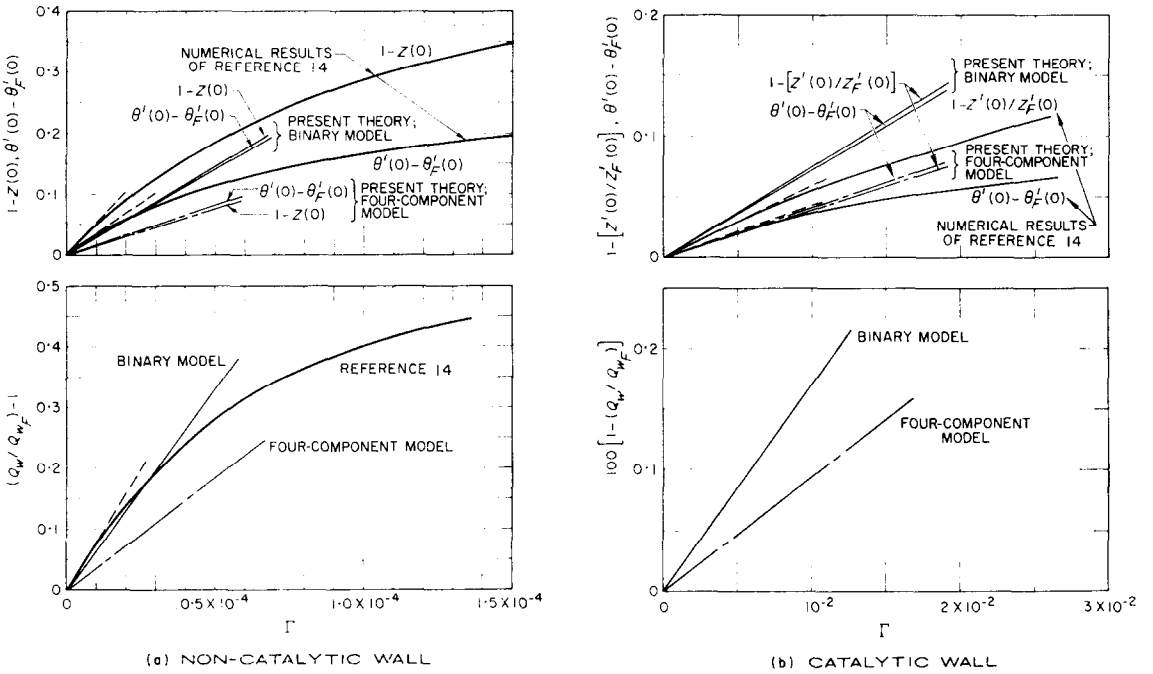

FIG. 5. Properties at the gas–surface interface for the stagnation point.

wall case, the agreement being best for the heat transfer. The corresponding agreement for the catalytic wall case is only fair.† The discrepancy between the present solution and that of Fay and Riddell for very small Γ is due to the simplifying assumptions $f \simeq f_B(\eta)$, $\rho\mu =$ constant and $\overline{c_P} =$ constant employed here which were not used in [14]. Clearly, the error in these assumptions is negligible for the purpose of calculating nonequilibrium heat transfer. It is of interest to note from Fig. 5 that the first-order theory is restricted in application to deviations from frozen flow on the order of 10 per cent or less; for $\Gamma \gtrsim 5 \times 10^{-5}$, the second ($\sim\Gamma^2$) and higher order effects which constitute a subtractive correction to the first-order theory become increasingly important.

Comparison of the results for the four-component mixture and the binary gas approximation for air indicates that the first-order nonequilibrium perturbations predicted by the latter model are roughly *twice* the four-component mixture values in the present example. This is because the binary model for air overestimates the total atom recombination rate near the highly cooled wall by approximately the factor $(\alpha_{2_e} + \alpha_{4_e})^2/(\alpha_{2_e}^2 + \alpha_{4_e}^2)$ (=1·91 in the present example).‡ Correspondingly, the temperature gradient and heat-transfer perturbations are also overestimated with the binary model by approximately the factor $(\alpha_{2_e} H_{D_2} + \alpha_{4_e} H_{D_4})(\alpha_{2_e} + \alpha_{4_e})/(\alpha_{2_e}^2 H_{D_4} + \alpha_{4_e}^2 H_{D_4}) = 1{\cdot}79$. Thus it is clear that the binary gas model of dissociated air, although undoubtedly a useful tool for rough engineering solutions, can overestimate the gas phase recombination effects near the wall by a factor of two for highly nonequilibrium stagnation point boundary layers when a significant concentration of the nitrogen as well as oxygen atoms exists at the edge of the

† Comparison of the catalytic wall heat-transfer perturbations, which are extremely small, has been omitted in Fig. 5(b), because of the difficulty in accurately determining Q_w/Q_{w_F} at very small Γ from the results given in [14].

‡ This can readily be seen by comparing $\dot{w}_2 + \dot{w}_4$ with $\dot{w}_Z$ from (14), using (9), (10) and neglecting the exponential dissociation rate terms near the wall.

boundary layer.† In this connection, the present analysis suggests that the binary-model solutions can be easily corrected to account for the multicomponent effects in air (at least for nearly frozen flows) by using the following effective recombination rate parameters $\bar{\Gamma}_\alpha$ and $\bar{\Gamma}_\theta$ in correlating the nonequilibrium effects on the specie and energy variables, respectively:

$$\left.\begin{aligned} \bar{\Gamma}_\alpha &\simeq \Gamma\left[\frac{\alpha_{2_e}^2 + (\lambda_4/\lambda_2)\,\alpha_{4_e}^2}{\alpha_e^2}\right] \\ \bar{\Gamma}_\alpha &\simeq \Gamma\left[\frac{\alpha_{4_e}^2 H_{D_2} + (\lambda_4/\lambda_2)\,\alpha_{4_e}^2 H_{D_4}}{\alpha_e(\alpha_{2_e} H_{D_2} + \alpha_{4_e} H_{D_4})}\right] \end{aligned}\right\} \quad (37)$$

which include (approximately) the effect of different species catalytic efficiencies for gas phase recombination with respect to either type of atom present. These parameters might have been deduced intuitively from an inspection of the original reaction rate terms, and also might be expected to hold as an approximation over a rather wide range of Γ values. Indeed, correlation rules of this type deduced empirically have been found to accurately describe stagnation point heat transfer to a perfectly non-catalytic wall over a large part of the entire nonequilibrium flow regime for a wide range of free flight conditions [1].

To conclude this discussion of stagnation flow, it is of interest to examine the sensitivity of the nonequilibrium heat transfer to the recombination rate exponent ω. Although earlier experimental investigations suggested the value $\omega = -1{\cdot}5$ for air and most diatomic gases (which value has been widely used in analyzing viscous and inviscid nonequilibrium flow problems), some recent studies [8, 54] indicate that ω might be more nearly between $-1{\cdot}0$ and $-0{\cdot}50$. Since the value of this parameter over the wide temperature range encountered across highly cooled stagnation boundary layers is therefore still uncertain, there arises the question as to the sensitivity of the nonequilibrium boundary-layer properties to the assumed value of ω. Now, this can be appraised (at least for small Γ) from the present theory using the following relation [see equations (12) and (17)]:

$$\Delta P = P - P_F \sim \Gamma\mathscr{I}(\infty) \sim \left(\frac{T_e}{T_{R_2}}\right)^{\omega-2} \mathscr{I}(\infty, \omega, \theta_w) \quad (38)$$

where P is any surface property (atom concentration, heat transfer, etc.). For $T_{R_2} = 4500°\text{K}$ [31] using the computed values of $\mathscr{I}(\infty, \omega, \theta_w)$ [52], the ratio $\Delta P(\omega)/\Delta P(\omega = -1{\cdot}5)$ for noncatalytic wall heat transfer is plotted as a function of ω in Fig. 6 for several different wall

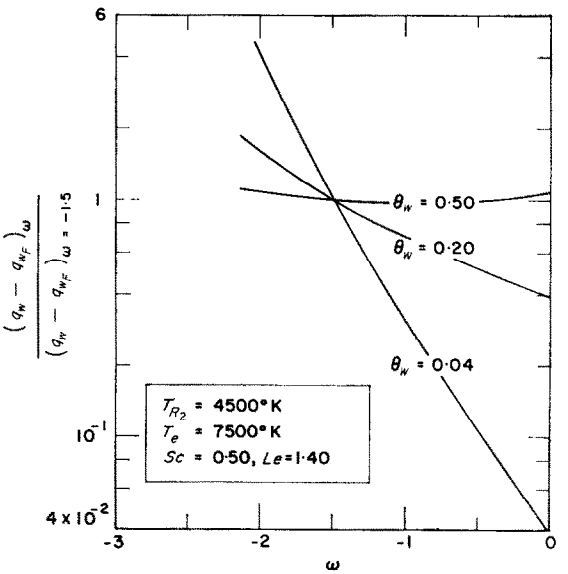

FIG. 6. Effect of recombination rate exponent on nonequilibrium stagnation point heat transfer.

temperature ratios and a typical stagnation temperature $T_e = 7500°\text{K}$. The heat-transfer perturbation due to nonequilibrium reaction is clearly very sensitive to the assumed value of ω for very highly cooled walls ($\theta_w \leqslant 0{\cdot}10$); changing ω from $-1{\cdot}5$ to $-1{\cdot}0$, for example, can reduce this perturbation by a factor of 3. However, with increasing wall temperature, the sensitivity to ω diminishes rapidly and is.

† Note from Fig. 5 that the errors introduced by neglecting the multicomponent effects on the reaction rate terms can be comparable to the combined error due to neglecting the details of the specific heat variations and transport properties, especially in the catalytic wall case.

negligible at $\theta_w = 0{\cdot}50$ in the present example.† This sensitivity to ω in the highly cooled wall case can perhaps serve as a means of measuring ω itself through direct catalytic–non-catalytic differential heat-transfer probe measurements and use of an accurate nonequilibrium boundary-layer theory, provided that the energy in dissociation is large enough and that equilibrium at the edge of the boundary layer can be at least approximately maintained [8].

B. *Hypersonic flow over a plate*

Hypersonic flow over a sharp, flat plate aligned with the incident stream ($Q = \kappa = 1$) provides a convenient physical model to illustrate the effects of nonequilibrium reaction on boundary layer flows around slender aerodynamic bodies. Here, viscous dissipation heating within the boundary layer initiates a dissociative reaction due to the large frozen flow temperature peak at the leading edge, and a dissociation-controlled relaxation toward equilibrium takes place with increasing distance along the plate.

Typical distributions of total atom concentration and temperature across the boundary layer near the leading edge of a highly cooled plate immersed in a low-temperature, equilibrium, hypervelocity stream of air are presented in Fig. 7 as a function of the local reaction parameter

$$\Gamma_D \equiv \left(\frac{T_e}{T_{R_1}}\right)^{-s_2} \left(\frac{T_e}{T_{R_2}}\right)^{2-\omega} \frac{\bar{\lambda}_2 p_{D_2}}{4p_e}\,\Gamma$$

$$= 2\bar{\lambda}_2\, k'_{R_{22}}\, Sc \left(\frac{p_0}{\mathscr{R}_u T_{R_2}}\right)^2 \exp A_2 \cdot \left(\frac{p_e}{p_0}\,\frac{x}{\kappa u_e}\right) \qquad (39)$$

(The reason for choosing this parameter is explained below.) These curves illustrate how the degree of dissociation and temperature increase and decrease, respectively, with distance along the plate due to the dissociation rate-controlled nonequilibrium relaxation process. Although the surface catalyticity has a pronounced effect on the atom concentration profile near the wall through the specie equation boundary conditions, it does not sensibly

† Although the effect of ω shown here is strictly applicable only to slightly unfrozen nonequilibrium flow, it has been shown to hold with good approximation throughout most of the nonequilibrium flow regime as well [55].

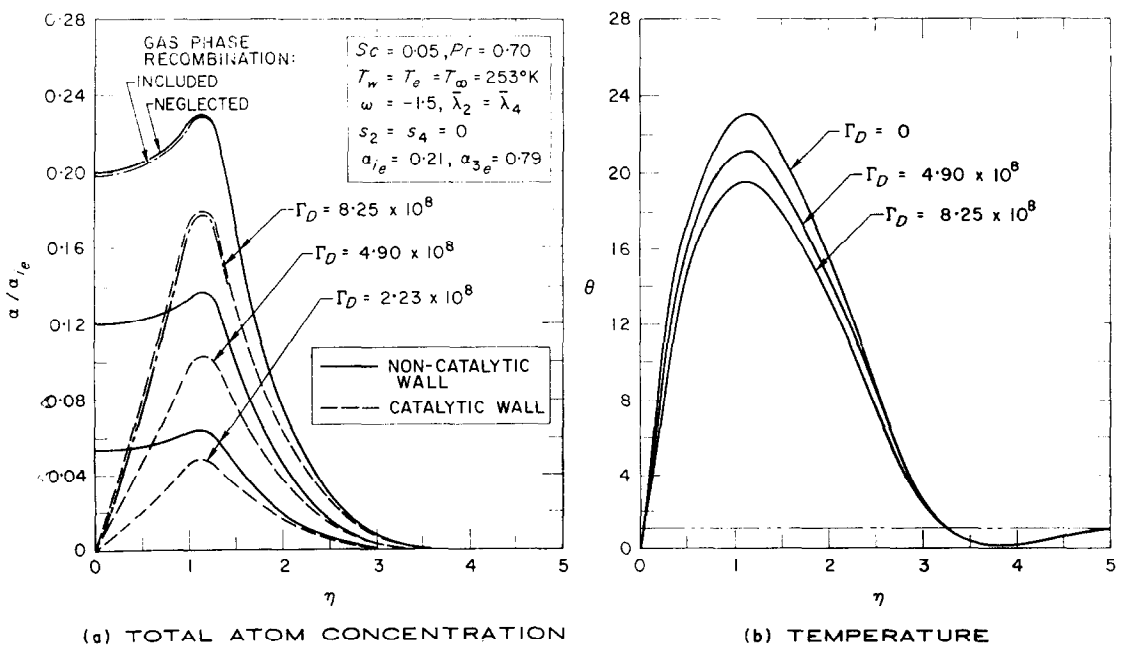

(a) TOTAL ATOM CONCENTRATION (b) TEMPERATURE

FIG. 7. State profiles across a hypersonic nonequilibrium boundary layer along a sharp flat plate.

affect the influence of the *gas phase* reaction on $a(\eta)$ in the region $0 \leq \eta < \eta^*$ because the solution is still completely dissociation rate-controlled for either a catalytic or non-catalytic wall. Indeed, this situation holds true throughout most of the relaxation region along the plate, until the boundary layer approaches close enough to equilibrium that the recombination rate in the gas near the surface becomes comparable to the local maximum dissociation rate [19, 20].

Some important aspects of the nonequilibrium boundary-layer behavior in highly dissipative flows are conveniently brought out by examining the first-order maximum total atom concentration solution $a(\eta^*)$ in more detail. Employing the relationships $\dot{w}_i = 0$ from equations (8) in (17) and (28) so as to eliminate a_{2_e} and a_{4_e} in favor of p_e, T_e and the molecule concentrations a_{1_e} and a_{3_e}, this solution can be written

$$
\begin{aligned}
a(\eta^*) - a_F(\eta^*) = \Gamma_D \Bigg[- \left(\frac{T_e}{T_{R_1}}\right)^{s_2} \left(\frac{T_e}{T_{R_2}}\right)^{\omega-2} \exp(-\theta_{D_2})\, \mathscr{I}_2(\infty, a_{2_e} = 0) \Bigg] [1 - a_F(\eta^*)]\, s(\eta^*) \\
\times \left\{ 1 + J \left[\frac{I_s(\eta^*, Sc)}{I_s(\infty, Sc)} - 1 \right] - \frac{\mathscr{I}_2(\eta^*)}{\mathscr{I}_2(\infty)} \right\} \left\{ \frac{0{\cdot}21 - a_{2_F}(\eta^*)}{1 - a_F(\eta^*)} \right. \\
\left. + \left[\frac{0{\cdot}79 - a_{4_F}(\eta^*)}{1 - a_F(\eta^*)} \right] \frac{\bar{\lambda}_4}{\bar{\lambda}_2} \frac{p_{D_4}}{p_{D_2}} \frac{[\theta_F(\eta^*)]^{s_4 - s_2}}{\sqrt{(\theta_{D_4}/\theta_{D_2})}} \exp\left[- \frac{(\theta_{D_4} - \theta_{D_2})}{\theta_F(\eta^*)} \right] \right\}
\end{aligned}
\tag{40}
$$

Here, it has been assumed that $\mathscr{I}_2(\eta^*)/\mathscr{I}_2(\infty) = \bar{\mathscr{I}}_2(\eta^*)/\bar{\mathscr{I}}_2(\infty) = \mathscr{I}_4(\eta^*)/\mathscr{I}_4(\infty)$ and the ratio $\mathscr{I}_4(\infty)/\mathscr{I}_2(\infty)$ evaluated from equation (31), which are very good approximations for dissociation rate controlled flows. This solution as it stands is generally applicable to either plate, wedge, or cone flows; the specialization to a particular case is made by selecting the appropriate values of κ and Q (e.g. $\kappa = Q = 1$ for the plate). The terms preceding the last braced expression in equation (40) pertain to the solution for the binary gas model based on pure oxygen properties, while the two terms inside the last braces represent the multicomponent species effects which are present in the case of a dissociating air mixture. Clearly, when $\theta_{D_4} \gtrsim 2\theta_{D_2} \gg 1$ and $p_{D4} \simeq 0(p_{D_2})$, $s_4 \sim 0(s_2)$ (as is the case for air), the last term in (40) may be neglected unless $\theta_F(\eta^*)$ is extremely large; this corresponds to the well-known physical fact that the nitrogen in air undergoes thermal dissociation only after the oxygen has first almost completely dissociated.

It is clear that Γ_D, instead of Γ, is the most appropriate (flow length/reaction length) parameter for dissociation rate controlled, nearly frozen nonequilibrium boundary-layer flows of either a pure diatomic gas or an air mixture with negligible nitrogen dissociation. Indeed, examination of the general nonlinear equations (2), (4) and (8) with the gas phase recombination terms ($\sim a_i^2$) neglected shows this to be the case regardless of the magnitude of the local dissociation rate. Consequently, equations (31), (39) and (40) together with the frozen flow solutions (23) and (24) show that the nearly frozen maximum atom concentration for a given gas and body shape depends only on the product $p_e x$ when u_e, a_{i_e}, T_e and the wall conditions are each fixed. [Again, it can be seen from the original governing equations of the problem with gas phase recombination neglected that this conclusion is not restricted to nearly frozen flow and, moreover, applies to $T(\eta)$ and each of the $a_i(\eta)$ for all η across the boundary layer.] This important similitude result is the expected consequence of the binary scaling principle due to Gibson [46, 56] as applied to hypersonic, dissociation rate controlled, nonequilibrium boundary-layer flows. A further simplification of the scaling rule obtains for sharp-nosed slender bodies with a small disturbance, hypersonic local inviscid flow ($u_e \simeq u_\infty$, $T_e \ll u_e^2/2\overline{c_P}$) when the temperature T_e has a comparatively small effect and can be dropped out of the similitude considerations. In this case, the effect of altitude at a fixed velocity and body

surface conditions in an undissociated free stream of given gas is completely scaled by a simple change in distance x according to $x \sim 1/p_e$ (with $p_e = p_\infty$ for the flat plate case). That is, the same values of $T(\eta)$ and $\alpha_i(\eta)$ occur at larger x with increasing altitude because of the reduction in the dissociation rate with dropping pressure.

In Fig. 8, some typical first-order variations of $\alpha(\eta^*)/\alpha_{1_e}$ along a non-catalytic plate are

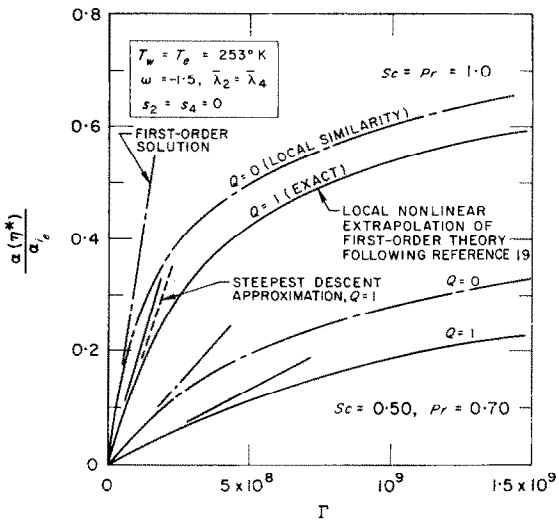

FIG. 8. Maximum atom concentration distribution along a non-catalytic plate for $M_\infty = 25$ at 200000 ft altitude.

plotted versus Γ_D for $Sc = Pr = 1$ and $Sc = 0{\cdot}50$, $Pr = 0{\cdot}70$, along with the result based on the steepest descent approximation for the $Sc = Pr = 1$ case. To indicate the limitations of the nearly frozen theory, there are also shown the corresponding nonlinear relaxation effects as obtained by a local nonlinear extrapolation of the first-order results according to the approximate theory of Rae [19]. It is seen that the steepest descent approximation yields a very accurate solution, only slightly underestimating the initial growth in the maximum atom concentration along the plate. It is also seen that the nonlinear relaxation effects become appreciable when $\alpha(\eta^*)/\alpha_{1_e} \gtrsim 0{\cdot}10$, which is to be expected since the first-order theory applies only at very small Γ_D. However, the extreme sensitivity to the transport property parameters observed in Fig. 8 is somewhat surprising at first; the initial gradient in $\alpha(\eta^*)$ along the plate for $Sc = Pr = 1$ is an order of magnitude larger than that predicted assuming $Sc = 0{\cdot}50$, $Pr = 0{\cdot}70$. A careful study of equations (24) and (40) shows that this is mainly due to the effect of the Prandtl number on the maximum frozen temperature as magnified by the exponential temperature function in the dissociation rate. Clearly, solutions based on the classical simplifying assumption $Pr = 1$ of boundary-layer theory will significantly overestimate the degree of dissociation in highly nonequilibrium air plate boundary layers ($Pr \approx 0{\cdot}70$). More generally, it can be inferred that a fairly detailed consideration of the effect of the transport properties across the boundary layer in dissociation-controlled flows (e.g. plates or slender cones) must be made to obtain nonequilibrium solutions of acceptable engineering accuracy.

In Fig. 8, there are also presented solutions based on the value $Q = 0$ instead of unity for the plate. Since $Q = (\xi/\Gamma)(d\Gamma/d\xi)$, these solutions therefore correspond to the assumption of local similarity whereby the non-similar effect of reaction is neglected *a priori*. It is seen that the local similarity approximation overestimates the initial atom concentration gradient along the plate by a factor of 2 in these examples. This approximation is clearly a poor one under very low ambient density conditions where the boundary layer remains nearly frozen (or almost so) over an appreciable extent of the plate. On the other hand, when the nearly frozen flow regime is confined to a small region near the leading edge, as is more often the case in practical problems, local similarity would appear to be a useful engineering approximation over most of the plate where nonlinear reaction effects predominate [28, 29]. It is noted from Fig. 8 that the accuracy of the local similarity solution is noticeably better for $Pr = Sc = 1$ than in the case where $Sc = 0{\cdot}50$, $Pr = 0{\cdot}70$ and hence depends to some extent on the transport properties.

The nonequilibrium heat-transfer distributions along the plate corresponding to the conditions in Fig. 8 are plotted in Fig. 9 for both non-catalytic and catalytic surfaces. The exact solutions with $Q = 1$ show the usual large

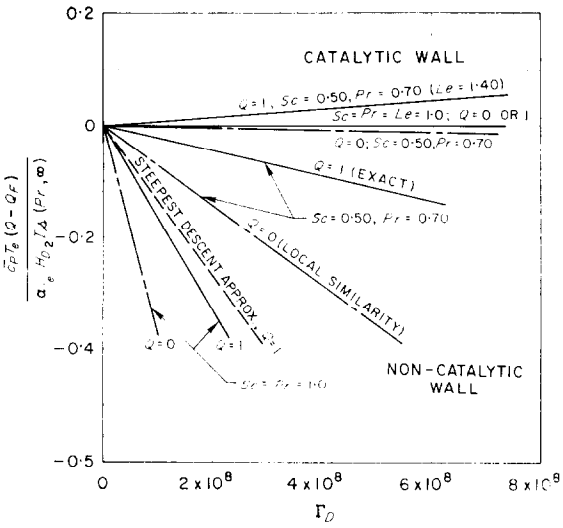

FIG. 9. First-order nonequilibrium heat-transfer distributions along the plate.

difference between non-catalytic and catalytic heat transfer for nonequilibrium flow. The nearly frozen non-catalytic heat transfer drops significantly with increasing distance along the plate because the growing atom concentration at the wall increasingly reduces the local overall driving enthalpy difference for heat transfer across the boundary layer. In contrast, for $Le > 1$, the heat transfer to a completely catalytic wall increases very gradually along the plate in the nearly frozen regime, since the growing local heat release to the wall due to heterogeneous atom recombination slightly exceeds the corresponding reduction in local heat conduction from the gas to the wall. As expected from the results of Fig. 8, the non-catalytic heat transfer is quite sensitive to the transport property parameters, the initial rate of decrease in heat transfer along the plate for $Sc = Pr = 1$ being five times greater than that for the case $Sc = 0{\cdot}50$, $Pr = 0{\cdot}70$. Thus, a detailed consideration of transport properties in the nonequilibrium boundary layer appears necessary for accurate engineering calculations of heat transfer as well as state profiles along the plate. This is in marked contrast to the stagnation point, where the nonequilibrium heat-transfer calculation is comparatively insensitive to the detailed transport property values. Clearly, experimental studies involving either absolute non-catalytic or differential non-catalytic–catalytic heat-transfer measurements on plates or slender cones with dissociation rate-controlled nonequilibrium boundary-layer flows should use theoretical solutions based on a careful consideration of the transport property variations *for these particular geometries.*†

A comparison of the exact ($Q = 1$) and locally similar ($Q = 0$) solutions in Fig. 9 indicates that the latter overestimates the initial gradient in heat transfer by a factor of three (as compared to the twofold overestimate of $\alpha(\eta^*)/\alpha_{1_e}$ shown in Fig. 8). Although the approximation improves considerably in the nonlinear relaxation region further downstream of the leading edge and is undoubtedly useful for rough engineering estimates, it may well not be a sufficiently accurate solution for the purpose of the aforementioned nonequilibrium heat-transfer studies.

C. *Slender cones in hypersonic flow*

To conclude the discussion of applications, we consider hypersonic flow over sharp cones with emphasis on the possibility of obtaining solutions by an appropriate scaling of the foregoing flat plate solutions. Now, under the conditions of small disturbance hypersonic flow appropriate for slender cones, the nonequilibrium boundary-layer behavior in the similarity co-ordinates is qualitatively the same as that for the plate. Obviously, there is an appreciable quantitative difference between the two at fixed flight velocity and wall conditions in a given gas because of the higher inviscid pressure and the Mangler factor $\kappa = 3$ (instead of unity) pertaining to the cone. Both of these effects are explicitly contained in the parameter Γ_D and thus simply accounted for by an appropriate scaling of the flat plate solution. In addition, however, there remain two features of the governing differential equations for the cone boundary layer which cannot be simply scaled

† This point has also been stressed by Hartunian and Marrone [9] in connection with their work on measuring transport properties of dissociated gases by heat-transfer measurements in shock tube boundary layers.

in this manner: (a) the nonequilibrium parameter derivative factor is $Q = 1/3$ instead of unity; (b) the higher invsicid flow temperature ($T_e > T_\infty$) for the cone gives a higher maximum boundary-layer temperature and thus a larger nonequilibrium dissociation rate. Under small disturbance hypersonic flow conditions for slender cones, the latter effect is usually presumed small and discarded *a priori* from similitude considerations; however, strictly speaking, it does remain, consistent with the assumption $u_e \simeq u_\infty$, and will be evaluated here. The former parameter Q brings in a basic body shape factor for the nonequilibrium boundary layer in addition to the body shape effects that can be explicitly scaled through the parameter Γ_D.

The significance of the effects (a) and (b) can be appreciated from Fig. 10, where some exact and locally similar first-order solutions for $\alpha(\eta^*)$ along 5 deg and 10 deg non-catalytic cones with a frozen inviscid flow [57] are compared with corresponding solutions for the flat plate. In this figure, all these solutions would coincide if the effects (a) and (b) above are both negligible. A comparison of the plate and cone solutions for $Q = 0$ indicates that the effect of $T_e > T_\infty$ on the cone solutions is indeed small and can be neglected regardless of the transport parameters assumed. It is noted, however, that the small error involved does tend to grow with increasing cone angle and for sufficiently large values of δ would eventually become significant (such that T_e could no longer be dropped from similitude considerations). Comparison of the exact solutions for the cone and plate shows that the influence of the body shape through the factor Q has a significant effect on the initial gradient of $\alpha(\eta^*)$ along the body, the first order cone solutions being roughly a factor of two higher than the plate values. Thus, under flight conditions where the nonequilibrium boundary layer remains nearly frozen over an appreciable extent of the cone, scaling from plate to cone according to the simple rule $\Gamma_{D_{\text{cone}}} = \Gamma_{D_{\text{plate}}}$ will not give accurate results since it significantly underestimates $\alpha(\eta^*)$ along the cone. By analogy

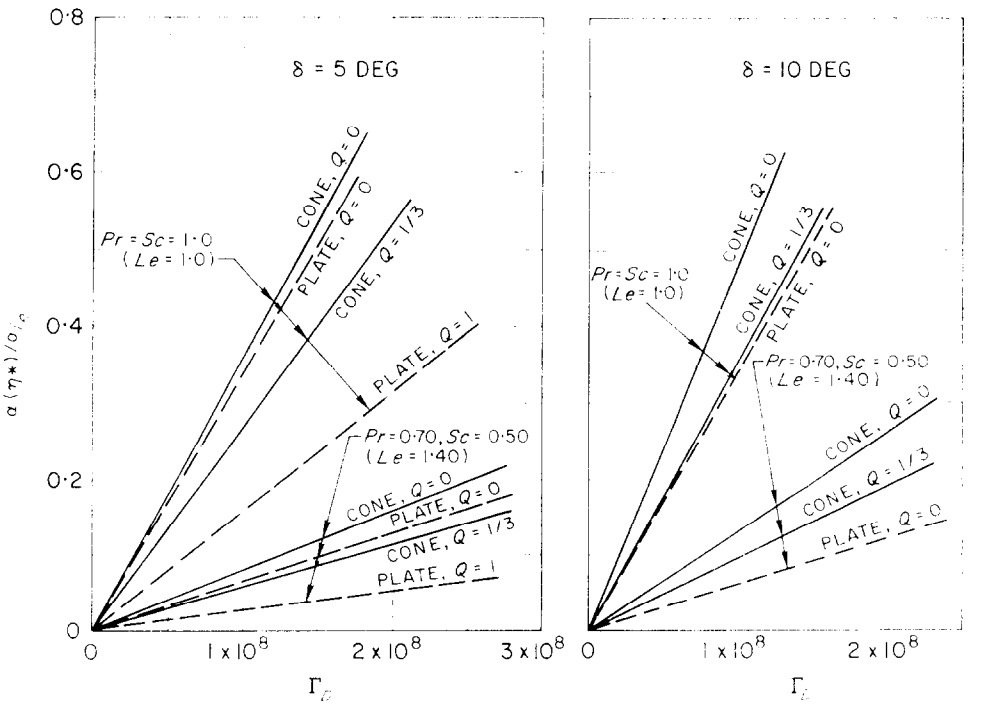

FIG. 10. Comparison between atom concentration solutions for a non-catalytic flat plate and slender cones.

with the results shown in Fig. 8, however, it is clear that the agreement between the exact cone and plate solutions is much better when a highly nonlinear relaxation region extends along much of the body; the $\Gamma_D = \text{constant}$ scaling procedure is probably a reasonable engineering approximation under such conditions.

It should be noted from Fig. 10 that the local similarity approximation for the slender cone is significantly better than the same approximation for the flat plate. This is to be expected when the effect of $T_e > T_\infty$ is very small, since the value of Q for the cone is closer to zero than is the value $Q = 1$ for the plate. Consequently, a good approximation for slender cones under all conditions, regardless of the transport parameter values, can be obtained by scaling via Γ_D the *locally similar solution* of the flat plate. That is, the solutions for $T(\eta)$ and $\alpha_i(\eta)$ for $Q = 0$ at some distance x_{plate} along the plate can be applied to any slender cone at a distance along the cone given by

$$x_{\text{cone}} \simeq \frac{3}{(p_e/p_\infty)_{\text{cone}}} x_{\text{plate}} \tag{41}$$

for a given gas at fixed velocity, wall temperature and catalycity, and ambient gas composition. In hypersonic flow where $p_e/p_\infty > 3$ (which is usually the case of interest), a shorter distance along the cone than along the plate is thus required to reach a given dissociation level.

V. SUMMARY

In this paper, a family of analytical solutions has been given for nonequilibrium boundary-layer flow of a four-component dissociating gas mixture, assuming small departures from frozen flow behavior and either a completely catalytic or perfectly non-catalytic body surface. Both recombination rate and dissociation rate controlled flow situations are included. Specific applications of the theory were discussed in some detail for highly cooled, self-similar stagnation point flow on blunt axisymmetric bodies and for the case of highly dissipative, non-similar boundary layers along a sharp flat plates and slender cones.

For the stagnation point flow, it was shown that formulation of the nonequilibrium chemical kinetics in air according to the binary "air atom–air molecule" approximation can overestimate the controlling gas phase recombination rate for the total atom concentration by a factor of two when an appreciable fraction of nitrogen as well as oxygen atoms exists at the edge of the boundary layer. A simple method of correcting these binary gas model solutions to account for the multicomponent mixture effects present in highly nonequilibrium-dissociated air was given. For highly cooled walls, it was also shown that the nonequilibrium heat transfer to a non-catalytic surface is quite sensitive to the value of the recombination rate temperature dependence exponent. This suggests that differential catalytic–non-catalytic heat-transfer measurements on nonequilibrium stagnation point boundary layers might be used to evaluate this exponent.

Examination of the flat plate and slender cone solutions brought out a number of important conclusions. First, in sharp contrast to the case of stagnation point flows, the surface catalycity was shown to have an altogether negligible influence on the effect of the gas phase reaction rate unless the boundary layer is rather close to complete equilibrium. Second, local similarity solutions were found to be reasonable engineering approximations for the flat plate when nonlinear relaxation effects predominate but were found to be poor approximations in regions where the boundary layer is nearly frozen. In contrast, local similarity yields fairly accurate results under all conditions for the case of slender cones. Third, the nonequilibrium boundary-layer solutions for both the plate and cone were shown to be very sensitive to the transport property parameters, as evidenced by the fact that the nearly frozen maximum atom concentrations decrease by an order of magnitude when Pr and Sc are changed from unity to 0·70 and 0·50, respectively. This result is in marked contrast to what is observed for recombination rate-controlled, nonequilibrium boundary layers such as at a stagnation point. Thus, it was concluded that a fairly detailed consideration of the transport properties across the boundary layer must be made to obtain solutions of acceptable engineering accuracy for dissociation rate-controlled flows.

Finally, a simple and unified nonequilibrium boundary-layer binary scaling law was demonstrated for plates and slender cones with a small disturbance hypersonic inviscid flow. This law provides that under conditions of fixed flight velocity, wall temperature, surface catalycity and free stream composition, the nonequilibrium properties across the boundary-layer scale along the body according to the simple rule $(\rho_e/\rho_\infty)\ [x/(1 + 2\epsilon)] = \text{constant}$. Thus, the effect of changing altitude on either the plate or cone solutions is easily evaluated, and solutions for slender cones are simply obtained from the flat plate by an appropriate local scaling of distance along the body.

REFERENCES

1. G. GOODWIN and P. M. CHUNG, Effects of nonequilibrium flows on aerodynamic heating during entry into the earth's atmosphere from parabolic orbits, *Advances in Aeronautical Sciences*, Vol. 4, pp. 999–1018. Pergamon Press, New York (1961).
2. R. J. WHALEN, Viscous and inviscid nonequilibrium gas flows, *J. Aerosp. Sci.* **29**, 1222–1237 (1962).
3. H. K. CHENG, Recent advances in hypersonic flow research, *Amer. Inst. Aeronaut. Astronaut. J.* **1**, 295–310 (1963).
4. N. T. GRIER and N. SANDS, Regime of frozen boundary layer in stagnation region of blunt reentry bodies. *NASA TN D*-865 (May 1961).
5. R. VAGLIO-LOURIN and M. H. BLOOM, Chemical effects in external hypersonic flows. *ARS* Preprint 1976–61 (August 1961).
6. D. E. ROSNER, Recent advances in convective heat transfer with dissociation and atom recombination, *Jet Propuls.* **28**, 445–451 (1958).
7. D. E. ROSNER, Scale effects and correlations in nonequilibrium convective heat transfer, *Amer. Inst. Aeronaut. Astronaut. J.* **1**, 1550–1555 (1963).
8. R. A. HARTUNIAN and W. P. THOMPSON, Nonequilibrium stagnation point heat transfer including surface catalysis. *Amer. Inst. Aeronaut. Astronaut.* Preprint 63–464 (August 1963).
9. R. A. HARTUNIAN and P. V. MARRONE, Viscosity of dissociated gases from shock-tube heat transfer measurements, *Phys. Fluids* **4**, 535–453 (1961).
10. D. E. ROSNER, Catalytic probes for the determination of atom concentrations in high speed gas streams, *J. Amer. Rocket Soc.* **32**, 1065–1073 (1962).
11. R. A. HARTUNIAN, Local atom concentrations in hypersonic dissociated flows at low densities, *Phys. Fluids* **6**, 343–348 (1963).
12. R. A. HARTUNIAN and S. W. LIU, Slow flow of a dissociated gas about a catalytic probe, *Phys. Fluids* **6**, 349–354 (1963).
13. R. A. HARTUNIAN, W. P. THOMPSON and R. B. SOLO, Measurements of surface catalytic efficiency and diffusion coefficient in a dissociated oxygen flow, *Bull. Amer. Phys. Soc. Series II* **8**, 494 (1963).
14. J. A. FAY and F. R. RIDDELL, Theory of stagnation point heat transfer in dissociated air, *J. Aero. Sci.* **25**, 73–85, 121 (1958).
15. J. E. BROADWELL, A simple model of the nonequilibrium dissociation of a gas in couette and boundary layer flows, *J. Fluid Mech.* **4**, 113–139 (1958).
16. P. M. CHUNG, A simplified study of the nonequilibrium couette and boundary layer flows with air injection. *NASA TN D*-306 (February 1960).
17. F. K. MOORE and W. J. RAE, The Rayleigh problem for a dissociated gas. *ARS* Preprint 1968–61 (August 1961). (Cornell Aeronautical Laboratory Report *AF*-1285-*a*-8, June 1961).
18. J. F. CLARKE, Energy transfer through a dissociated diatomic gas in couette flow, *J. Fluid Mech.* **4**, 441–465 (1958).
19. W. J. RAE, An approximate solution for the nonequilibrium boundary layer near the leading edge of a flat plate. *IAS* Preprint 62–178 (June 1962).
20. G. R. INGER, Nonequilibrium hypersonic boundary layer flow along a sharp flat plate with a strong induced pressure field. *AIAA* Preprint 63–442 (August 1963).
21. P. M. CHUNG and S. W. LIU, Simultaneous gas-phase and surface atom recombination for stagnation boundary layer, *Amer. Inst. Aeronaut. Astronaut. J.* **1**, 929–931 (1962).
22. A. LIÑAN and I. DA RIVA, Chemical nonequilibrium effects in hypersonic aerodynamics. Third International Congress on Aeronautical Sciences, Stockholm, Sweden, *ASTIA AD* 294–638 (August 1962).
23. G. R. INGER, Nonequilibrium stagnation point boundary layers with arbitrary surface catalycity, *Amer. Inst. Aeronaut. Astronaut. J.* **1**, 1776–1784 (1963).
24. S. M. SCALA, Hypersonic stagnation point heat transfer to surfaces having arbitrary catalytic efficiency, *Proc. U.S. Nat. Congr. Appl. Mech.* 799–806, American Society of Mechanical Engineers, New York (1958).
25. P. M. CHUNG and A. D. ANDERSON, Dissociation relaxation of oxygen over and adiabatic flat plate at hypersonic mach numbers. *NASA TN D*-190 (April 1960).
26. P. M. CHUNG and A. D. ANDERSON, Heat transfer around blunt bodies with nonequilibrium boundary layers. *Proc.* 1960 *Heat Transfer and Fluid Mechanics Inst.* pp. 150–163. Stanford University Press, California (1960).
27. J. A. MOORE and A. PALLONE, Similar solutions to the laminar boundary layer equations for nonequilibrium air. AVCO Corp., *RAD TM*-62-59 (July 1962).
28. F. G. BLOTTNER, Chemical nonequilibrium boundary layer. *AIAA* Preprint 63–443 (August 1963).
29. E. S. LEVINSKY and J. J. BRAINERD, Inviscid and viscous hypersonic nozzle flow with finite rate chemical reactions. *AEDC TRD*-63-18 (January 1963).

30. A. PALLONE, J. MOORE and J. ERDOS, Nonequilibrium, nonsimilar solutions of the laminar boundary layer equations. AVCO Corp., *RAD TM*-63-58 (August 1963).
31. J. D. TEARE, P. HAMERLING and B. KIVEL, Theory of the shock front, high temperature reaction rates. AVCO-Everett Research Lab. Note 133 (June 1959).
32. F. K. MOORE, Viscosity of dissociated air, *J. Amer. Rocket Soc.* **32**, 1415–1416 (1962).
33. L. LEES, Laminar heat transfer over blunt-nosed bodies at hypersonic flight speeds, *Jet Propulsion* **26**, 259–269 (1956).
34. L. LEES, Convective heat transfer with mass addition and chemical reactions, *Third AGARD Combustion and Propulsion Symposium*, pp. 451–498. Pergamon Press, New York (1958).
35. G. R. INGER, Dissociation-recombination nonequilibrium in the laminar hypersonic boundary layer, Ph.D. Dissertation, Dept. Aero/Astronautical Engineering, University of Michigan, May 1960 (University of Microfilms, Ann Arbor, Michigan).
36. D. E. ROSNER, Similitude treatment of hypersonic stagnation heat transfer, *J. Amer. Rocket Soc.* **29**, 215–216 (1959).
37. G. R. INGER, Specific heat inequality effect in the chemically frozen stagnation point boundary layer, *J. Amer. Rocket Soc.* **30**, 1028–1029 (1960).
38. P. M. CHUNG and A. D. ANDERSON, Heat transfer around blunt bodies with surfaces of finite catalytic efficiency in frozen dissociated hypersonic flow, *Advances in Astronautical Science* Vol. 8, pp. 188–197. Plenum Press, New York (1962). (*NASA TN D*-350, 1961.)
39. N. M. KEMP, P. H. ROSE and R. W. DETRA, Laminar heat transfer around blunt bodies in dissociated air, *J. Aerospace Sci.* **26**, 421–430 (1959).
40. F. K. MOORE, On local flat plate similarity in the hypersonic boundary layer, *J. Aerospace Sci.* **28**, 753–762 (1961).
41. P. M. CHUNG, Hypersonic viscous shock layer of nonequilibrium dissociating gas. *NASA TR R*-109 (1961).
42. G. R. INGER, Nonequilibrium-dissociated boundary layers with a reacting inviscid flow, *Amer. Inst. Aeronaut. Astronant.* **1**, 2057–2061 (1963).
43. R. GOULARD, On catalytic recombination rates in hypersonic stagnation heat transfer, *Jet Propuls.* **28**, 737–745 (1963).
44. D. E. ROSNER, Boundary conditions for the flow of a multicomponent gas, *Jet Propuls.* **28**, 555–556 (1958).
45. D. E. ROSNER, Chemical frozen boundary layers with catalytic surface reaction, *J. Aerospace Sci.* **26**, 281–286 (1959).
46. J. G. HALL, A. Q. ESCHENROEDER and P. V. MARRONE, Blunt-nose inviscid airflows with coupled nonequilibrium processes, *J. Aerospace Sci.* **29**, 1038–1052 (1962).
47. E. R. COLEMAN, and P. J. DOODY, On chemical processes in hypersonic shock layers, Bendix Systems Div. Report *BSR*-509 (March 1961).
48. K. L. WRAY, Cnemical kinetics of high temperature air, *Hypersonic Flow Research—Progress in Astronautics and Rocketry*, Vol. 7, pp. 181–204. Academic Press, New York (1962).
49. S. S. PENNER, *Chemistry Problems in Jet Propulsion*, pp. 216–232. Pergamon Press, New York (1957).
50. S. W. BENSON and T. FUENO, The mechanism of atom recombination by consecutive vibrational deactivations, *J. Chem. Phys.* **36**, 1597–1604 (1962).
51. E. D. RAINVILLE, *Intermediate Differential Equations*. John Wiley, New York (1943).
52. G. R. INGER, Highly nonequilibrium boundary layer flows of a multi-component dissociated gas mixture. Aerospace Corp. Report *TDR*-269(4230-10)-2 (October 1963).
53. P. M. MORSE, and H. FESHBACK, *Methods of Theoretical Physics*, Vol. 1, pp. 440–441. McGraw-Hill, New York (1953).
54. K. L. WRAY, Shock tube study of the recombination of O-atoms by Ar catalysts at high temperatures. AVCO-Everett Research Report 142 (September 1962).
55. G. R. INGER, Correlation of surface temperature effect on non-equilibrium heat transfer, *J. Amer. Rocket Soc.* **32**, 1743–1744 (1962).
56. W. E. GIBSON, Dissociation scaling for nonequilibrium blunt nose flows, *J. Amer. Rocket Soc.* **32**, 285–87 (1962).
57. M. F. ROMIG, Conical flow parameters for air in dissociation equilibrium. Convair Research Report 7, San Diego (May 1960).

Résumé—Des solutions analytiques sont présentées pour une famille d'écoulements du type couche limite d'un mélange gazeux dissocié de quatre constituants très éloigné de l'équilibre (presque figé) autour d'obstacles sans ablation avec une surface soit complètement catalytique soit parfaitement non-catalytique. A la fois, des écoulements en similitude et sans similitude locale sont étudiés pour des cas contrôlés soit, par la vitesse de recombinaison, soit, par la vitesse de dissociation. Le comportement d'une couche limite en dehors de l'équilibre, en tenant compte de la sensibilité aux différentes données de la cinétique chimique et aux paramètres de transport, est considéré en détail pour des écoulements au point d'arrêt d'obstacles arrondis fortement refroidis et des écoulement hypersoniques sur des plaques planes à bord aigu et des cônes élancés.

La précision de l'approximation de la similitude locale et l'emploi de lois d'échelle dans le cas binaire en déhors de l'équilibre sont examinés également pour les écoulements sur une plaque et sur un cône.

Zusammenfassung—Analytische Lösungen werden vorgelegt für eine Gruppe von Grenzschichtströmungen, die aus einem dissoziierten Gasgemisch mit vier Komponenten bestehen und sich weit ausserhalb des Gleichgewichtzustandes befinden. Sie erfolgen um Körper mit einer entweder vollkommen katalytischen oder vollkommen nicht-katalytischen Oberfläche. Die Körper sind so ausgebildet, dass sich die Strömung nicht ablöst. Sowohl ähnliche als auch örtlich verschiedene Strömungen werden untersucht für Zustände, in denen entweder die Vereinigungsrate oder die Dissoziationsrate vorherrscht. Das Verhalten der Grenzschichten ausserhalb des Gleichgewichtes, einschliesslich der Empfindlichkeit gegenüber verschiedener chemisch-kinetischer Werte und Parameter für die Transporteigenschaften, wird in Einzelheiten für stark gekühlte Strömungen am Staupunkt stumpfer Körper und für Überschallströmungen über scharfe flache Platten und schlanke Kegel betrachtet. Die Genauigkeit der örtlichen Ähnlichkeitsnäherung und die Anwendung der Gesetze für Zweistoffgemische ausserhalb des Gleichgewichtes werden ebenfalls für die Platten- und Kegelströmung geprüft.

Аннотация—В статье даются аналитические решения для некоторых весьма неравновесных (почти замороженных) четырехкомпонентных диссоциированных газовых смесей в пограничном слое неаблирующих тел с полностью каталитической или совершенно некаталитической поверхностью. Рассматриваются как автомодельные, так и локально неавтомодельные течения для случаев, когда определяющей является либо скорость рекомбинации, либо скорость диссоциации. Приводится подробный анализ неравновесного пограничного слоя, включающий его зависимость от различных химико-кинетических параметров и коэффициентов переноса применительно к задачам интенсивно охлаждаемой критической точки тупых тел и гиперзвуковых обтеканий плоской пластины и длинных конусов. Для пластины и конуса обсуждаются вопросы точности приближений локального подобия и неравновесности.